1

Theoretical and Physical Aspects of Nuclear Shielding

BY CYNTHIA J. JAMESON

A. General Theory — The general concept of nuclear shielding in the presence of electromagnetic radiation is introduced by defining dynamic electromagnetic shielding tensors which describe the linear response in an external spatially uniform periodic electromagnetic field.[1] The diamagnetic terms do not depend on the angular frequency, ω, of the electromagnetic radiation. The dynamic paramagnetic shielding tensor is a generalization of Ramsey's definition for the static property.

The magnetic field induced by the electrons at nucleus I is expressed by Lazzeretti and Zanasi as follows[1]:

$$\mathbf{B}_{\text{induced}} = -\left(\sigma^{p} + \sigma^{d}\right)\cdot\mathbf{B} - \hat{\sigma}^{p}\cdot\dot{\mathbf{B}} + \lambda^{I}\cdot\mathbf{E} + \hat{\lambda}^{I}\cdot\dot{\mathbf{E}} \qquad (1)$$

The external magnetic field $\mathbf{B}$ is the real part of $\mathbf{B}_0 \exp(i\omega t)$. $\dot{\mathbf{B}}$ is the partial derivative with respect to time. In the first term, σ^p is the dynamic paramagnetic shielding tensor,

$$\sigma^{p}(\omega) = \left(\frac{\mu_0}{4\pi}\right)\cdot\frac{-e^2}{2m^2\hbar}\sum_{j\neq a}\frac{2\omega_{ja}}{\omega_{ja}^2 - \omega^2} \times \mathrm{Re}\left(\langle a|\mathbf{M}_I|j\rangle\langle j|\mathbf{L}|a\rangle\right) \qquad (2)$$

in which $\mathbf{L}$ and $\mathbf{M}_I$ involve the usual angular momentum operators ℓ_i ($\mathbf{R}_I$) centered on I and ℓ_i at the gauge origin.

$$\mathbf{M}_I = \sum_i \frac{\ell_i(\mathbf{R}_i)}{|\mathbf{r}_i - \mathbf{R}_I|^3} \qquad \mathbf{L} = \sum_i \ell_i \qquad (3)$$

and $|a\rangle$ and $|j\rangle$ are the time-independent perturbed states which are functions of $\mathbf{B}_0$. σ^d is the same as Ramsey's, and the $\hat{\lambda}^I(\omega)$ term is called magnetoelectric shielding. Its physical meaning is shown in the equation; by taking the scalar diadic product with the time derivative of external electric field, one obtains the magnetic field induced at the nucleus. The terms in $\hat{\sigma}^p$ and λ^I give the magnetic fields induced at the nucleus by a time-dependent magnetic field and an external electric field, respectively. $\lambda^I(\omega)$ is the analogous definition to $\sigma^p(\omega)$, except that $\mathbf{L}$ is replaced by $-2mc\mathbf{R}$, $\mathbf{R}$ being $\sum_i \mathbf{r}_i$. $\hat{\sigma}^p(\omega)$ takes the imaginary part, whereas σ^p has the real part of the complex integrals $\langle a|\mathbf{M}_I|j\rangle\langle j|\mathbf{L}|a\rangle$ and $\hat{\lambda}^I$ takes the imaginary part, while λ^I has the real part of the complex integrals $\langle a|\mathbf{M}_I|j\rangle\langle j|\mathbf{R}|a\rangle$. The generalized

treatment shows fundamental relationships among the electromagnetic properties of molecules and the sum rules obeyed by them.[1]

The dispersion (dependence on ω) of the paramagnetic nuclear shielding in H_2O has been calculated and found to be significant. For example, for ^{17}O in H_2O, in ppm, with the gauge origin at the center of mass,

$$\sigma^p(\omega=0) = \begin{pmatrix} -111.806 & & \\ & -48.613 & \\ & & -103.779 \end{pmatrix} \quad (4)$$

$$\sigma^p(\omega=0.3 \text{ a.u.}) = \begin{pmatrix} -169.064 & & \\ & -421.457 & \\ & & -225.955 \end{pmatrix} \quad (5)$$

a downfield shift of 184 ppm! This theory predicts a frequency dependence of the dimensionless chemical shifts in NMR spectroscopy, analogous to the frequency dependence (dispersion) of the electric dipole polarizabilities.

Is there a possibility of measuring this dispersion of nuclear shielding by conventional NMR spectroscopy? The formalism developed by Lazzeretti and Zanasi is for a magnetic field **B**, which is the real part of $\mathbf{B}_0 \exp(i\omega t)$. In the NMR experiment the resultant applied magnetic field has a steady component B_0 (static uniform field) along the laboratory z axis and a component of amplitude B_1 rotating in the xy plane with angular velocity ω:

$$\mathbf{B} = \mathbf{B}_0 + \mathbf{B}_1(\omega, t) = \hat{k}B_0 + \hat{i}\,|B_1|\cos\omega t - \hat{j}\,|B_1|\sin\omega t \quad (6)$$

The radiation's magnetic field amplitude is related to the radiation intensity (related to rf transmitter power). Since $|B_1|$ is usually orders of magnitude smaller than B_0, the resultant **B** is very nearly equal to B_0 and very nearly along the z axis. Therefore, we could write the relevant part of $\mathbf{B}_{induced}$ as

$$-(\sigma^p(0) + \sigma^d(0))\cdot\mathbf{B}_0 - (\sigma^p(\omega) + \sigma^d(\omega))\cdot\mathbf{B}_1(\omega, t)$$

or

$$\sigma = \sigma^p(0) + \sigma^d(0) + [\sigma^p(\omega) - \sigma^p(0)]\,\frac{|B_1|}{B_0} \quad (7)$$

NMR spectrometers are now routinely available for observing ^{17}O at 67.8 MHz (500 MHz proton). ω = 1 a.u. corresponds to an energy of 1.0 hartree or $\omega/2\pi = 6.58 \times 10^{15}$ Hz. For ω = 0.3 a.u. or 1.97×10^{15} Hz, the calculated change is $[\sigma^p(\omega = 0.3 \text{ a.u.}) - \sigma^p(\omega = 0)] = 184 \times 10^{-6}$. For the time being let us assume that the dispersion is linear (linear dependence of σ^p on ω). Then the calculated change $[\sigma^p(\omega) - \sigma^p(0)]$ corresponds to a shielding change of $184 \times 10^{-6}(67.8 \times 10^6/1.97 \times 10^{15})$ $(|B_1|/B_0)$. This is far too small to detect for ^{17}O in H_2O. More favorable examples might be molecules having low-lying magnetic-dipole-allowed transitions from the ground state, that is, molecules with very large temperature-independent paramagnetism, such that ω_{ja} is small and closer to radiofrequencies. The frequency dispersion of the

nuclear shielding could be observed if ω_{res} is of the order of $10^{13} - 10^{14}$ Hz, that is, using $\mathbf{B}_0$ fields a factor of about 10^4 stronger. At such high fields, however, the higher order terms in

$$\sigma_{\alpha\beta} = \overset{(0)}{\sigma}_{\alpha\beta} + \frac{1}{6}\overset{(2)}{\tau}_{\alpha\beta\gamma\delta}\mathbf{B}_\gamma\mathbf{B}_\delta + \ldots \quad (8)$$

should be taken into consideration, as proposed by Ramsey,[2] i.e., the experiment would no longer be in the first-order Zeeman regime (see this series, Vol. 9, Chapter 1).

Another interesting development in fundamental theory of nuclear shielding has to do with the parity non-conservation (PNC). The PNC contribution to the nuclear magnetic shielding tensor has been derived,[3] based upon a transposition of the Ramsey theory using a molecular hamiltonian including PNC terms. There is no first-order contribution to σ from V_{PNC}. The only second-order PNC contribution comes from the molecular hamiltonian Larmor frequency term in $B_0 \cdot L$ and V_{PNC}. This contribution is a nine-component second-rank tensor, just as the parity-conserving shielding tensor derived by Ramsey. The magnitude of the PNC contribution increases roughly as Z^2. What this means is that a high Z nucleus in the right- and the left-handed optical isomers of an optically active molecule will have different *intrinsic* nuclear shielding. The NMR splitting which could be observed in two molecules of opposite chirality, owing to parity non-conservation, has been calculated for Tl in three compounds. The calculated splitting is 0.3×10^{-3} to 1.1×10^{-3}Hz at 288.5 MHz ^{205}Tl (i.e., 500 MHz proton). This is too small to detect. The chirality-dependent shielding of a sensor nucleus by a chiral perturbing group in the long-range limit, at a sufficiently large separation that there are no geometric correlations between a chiral solute molecule and a chiral solvent molecule, has been reviewed previously and likewise been shown too small.[4] Of course, there are larger well-known shifts between two molecules of opposite chirality in a chiral solvent due to differing geometry-imposed solute-solvent interactions. There is also the intramolecular counterpart of this. A carbon nucleus influenced by two chiral centers in the same molecule may experience different environments. These effects are not averaged even under unrestricted internal rotation.[5]

Reviews of nuclear shielding calculations have appeared.[6, 7]

B. *Ab Initio* Calculations. — The nuclear shielding differences between gaseous metal anions and neutral atoms were calculated for the alkali series Li through Cs by combining Hartree-Fock calculations with electron-electron correlation corrections.[8] The latter was obtained by applying the Hellmann-Feynman theorem to the nuclear charge-dependence of the correlation energy,

$$\sigma_{corr} = -\left(\frac{\mu_0}{4\pi}\right)\cdot\frac{1}{3}\left\{\frac{dE_{corr}(Z)}{dZ}\right\}_Z . \quad (9)$$

For the shielding difference $\sigma(M^-) - \sigma(M)$,

$$\sigma_{corr}(M^-) - \sigma_{corr}(M) = \left(\frac{\mu_0}{4\pi}\right) \cdot \frac{1}{3} \left(\frac{dI_{corr}(Z)}{dZ}\right)_Z \tag{10}$$

where $I_{corr}(Z)$ is the contribution arising from electron correlation, to the ionization potential for the removal of an electron from the system of nuclear charge Z and isoelectronic with M^- to yield a system isoelectronic with M.

$$I_{corr}(Z) = I_{expt}(Z) - I_{HF}(Z) - I_{rel}(Z) + \frac{I_{expt}(Z)}{m_M} \tag{11}$$

Relativistic contributions to the ionization potential have to be included, expecially for the heavier alkali, and the last term is the leading correction from nuclear motion for nuclear mass m_M. The numerical results are shown in Table 1.

Table 1. *Shielding Differences for Alkali Nuclei in the Free Ions*[8]

M	$\sigma(M^-)_g - \sigma(M)_g$	$\sigma(M^+)_g - \sigma(M)_g$
Li	3.14 ppm	– 6.07 ppm
Na	2.88	– 5.18
K	2.38	– 4.08
Rb	2.27	– 3.77
Cs	2.08	– 3.31

These results are for isolated neutral atoms and ions. Comparison with experiments has been made only in solutions where the M^- anion is stabilized by various solvents. The observed differences $\sigma(M^-)_{soln} - \sigma(M^+)_{aq}$ are compared with the $\sigma(M)_g - \sigma(M^+)_{aq}$ in order to obtain $\sigma(M^-)_{soln} - \sigma(M)_g$. The latter are compared with the calculations to show that Na^- interacts very weakly with its surroundings [(i.e., $\sigma(M^-)_{soln} - \sigma(M)_g \approx \sigma(M^-)_g - \sigma(M)_g$], whereas Rb^- and Cs^- are largely deshielded in solution relative to gaseous M^- anions.[8] MAS NMR spectra reveal that the Na^+ cation in $NaBPh_4$ crystal is very similar to gaseous Na^+ ion, whereas large deshielding is observed in a number of inorganic salts, showing a range of about 60 ppm. The shifts depend on variety of ligand molecules (H_2O, ether, or carbonyl) and Na–O interatomic distances, but are independent of the type of counter ion.[9]

^{31}P nuclear shielding calculations in PH_3, P_4, P_2, PN, PF_3, PF_4^+, PF_5, PF_6^-, and PO_4^{3-} have been reported.[10, 11] A basis set which is triple zeta plus two sets of d polarization functions (66211/6211/11) = [5s, 4p, 2d] appears to be adequate for the series HCl, H_2S, PH_3, SiH_4 when the GIAO-FPT method is used.[12] Comparisons with other theoretical calculations and experiment are shown in Table 2.

The GIAO-FPT calculations using this intermediate-size basis set[12] give very good agreement with experiment, at least as good as the earlier common-origin CHF.

Table 2. *Heavy Atom Shielding for Second-Row Hydrides, ppm*

σ	CF[12]	Expt	HL[13]	LZ[14]	KA[15]
^{35}Cl in HCl	948.4	952[16-18]	939.0	945.2	
^{33}S in H_2S	713.1	752[19]	718.5	704.3	
^{31}P in PH_3	598.1	597[20, 18]	584.9	577.6	589.6
^{29}S in SiH_4	499.5		480.9	472.2	
$\sigma_{//} - \sigma_{\perp}$					
^{35}Cl in HCl	301.4	292[16-18]	314.9	305.7	
^{33}S in H_2S	301.6		313.9	325.3	
^{31}P in PH_3	–32.8	–55,[21] –52[20, 18]	–36.4	–39.8	–38.8

calculations using larger basis sets.[13-15] The latter method has been applied to ^{31}P shielding in PF_3, PF_4^+, PF_5, PF_6^-, PO_4^{3-}, P_4, P_2, and PN.[10, 11] The results are shown in Tables 3 and 4. The molecules P_2 and P_4 are at the extremes of the ^{31}P shielding scale, only the free P atom (961.1 ppm)[22] is known to be more shielded than P_4.

Table 3. *^{31}P Shielding Calculated by Conventional CHF[10, 11] and Compared with Experiment, ppm*

	$\sigma_{//}$	Expt	$\sigma_{\perp}$	Expt	σ_{av}	Expt	$\sigma_{//}-\sigma_{\perp}$	Expt
PN	966	970	–497	–406	–10	53[a]	1463	1376[a]
P_2	969.1		–933.5		–299.3		1902.6	
PF_3	543.4	357	298.7	175	372.5	236[b]	244.7	182[b]
PF_5	490		623		580.7	436[c]	– 133	

[a] Ref. 23; [b] Ref. 24; [c] Ref. 25.

Table 4. *^{31}P Shielding Calculated by Conventional CHF[10, 11] and Compared with Experiment, ppm*

	σ_{av}	Expt	$\sigma_{//}-\sigma_{\perp}$	Expt
P_4	885.0	806-878[a]	–357.1[b]	–405[c]
PF_4^+	515.4[f]			
PF_6^-	673.3[f]	500[d]		
PO_4^{3-}	495.9	344[e]		

[a] Based on absolute shielding of ^{31}P in PH_3 = 595 ppm, from which is obtained σ(H_3PO_4 std. ref) = 356 ppm,[26] and σ(P_4) – σ(H_3PO_4) = 462 ppm in solid P_4,[27] 511 ppm in P_4 inf. dil. in CS_2,[28] and 522 ppm in P_4 inf. dil. in benzene[28]; [b] The parallel direction is the vector from the P nucleus to the center of the tetrahedral cluster; [c] Ref. 29; [d] in KPF_6 solution in acetonitrile[30]; [e] in $K_3PO_{4(s)}$[31]; [f] Assumed R_{PF} = 1.58 Å for PF_6^- and 1.445 for PF_4^+.

Calculations of ^{29}Si shielding[32] in molecules which are typical counterparts of the CH_4, C_2H_6, $CH_2{=}CH_2$ and $H_2C{=}O$ molecules indicate that the trends in σ for the Si compounds are much like that observed for the carbon compounds, as shown in Table 5.

Table 5. *Comparison of ^{29}Si Shielding with ^{13}C Shielding in Analogous Molecules, ppm*

^{13}C	$\sigma-\sigma(CH_4)$	Expt[a]	^{29}Si	$\sigma-\sigma(SiH_4)$[b]	Expt
CH_4	0	0	SiH_4	0	0[e]
C_2H_6	–9.6[c]	–14.3	Si_2H_6	21.4	12[f]
$H_2C{=}CH_2$	–135.4[c]	–130.6	$H_2Si{=}SiH_2$	–134.0	–157[g]
$H_2C{=}O$	–206.2[d]	–205	H_2SiO	–152.4	

[a] See this series, Vol. 16, Chapter 1, Table 1 for references; [b] Ref. 32; [c] Conventional CHF calculations, Ref. 33; [d] Ref. 34; [e] σ(TMS, liq) – $\sigma(SiH_4)$ = –91.9 ppm[35]; [f] Ref. 36; [g] Value for $(mes)_2Si{=}Si(mes)_2$.[37]

The ^{29}Si shielding tensor components from these conventional CHF calculations using large basis sets, gauge origin at Si, are shown in Table 6.

Table 6. *Calculated ^{29}Si Shielding, ppm*[32]

	σ_{xx}	σ_{yy}	σ_{zz}	σ_{av}
SiH_4				479.8[d]
Si_2H_6[a]	308.7	308.7	486.2	501.2
$H_2Si{=}SiH_2$[b]	467.0	176.0	394.5	345.2
H_2SiO[c]	374.0	132.8	475.5	327.4

[a] D_{3h} symmetry assumed, z axis along Si–Si; [b] z axis along Si=Si, y axis in molecular plane; [c] z axis along Si=O, y axis in molecular plane; [d] This may be compared with other calculations: 481.8 ppm,[13] 472.2 ppm,[14] by conventional CHF and 499.5 ppm[12] by GIAO-FPT.

The sagging pattern observed in the ^{29}Si shielding in the series SiH_nF_{4-n} has been reproduced by conventional CHF calculations[38]:

	SiH_4	SiH_3F	SiH_2F_2	$SiHF_3$	SiF_4
σ_{av}, ppm	479.8[32]	430.9	457.2	510.8	556.[39]
$\sigma-\sigma$(TMS)[36]	–93.1, –91.9	–17.4	–28.5	–77.8	–109.0, –113.6

The basis set used in these calculations is of the same quality as in Refs. 32 and 39. With the Si nucleus as the gauge origin, the diamagnetic contribution increases linearly with F substitution in going from SiH_4 to SiF_4, but the paramagnetic

contribution is a curve with the highest (smallest negative) value at SiH_4, dropping markedly with the first F substitution and changing only slightly with additional replacement of H with F atoms. This trend in the paramagnetic contribution has been previously predicted by Radeglia et al., based on semiempirical calculations and analyses of the dependence of ^{29}Si shielding on effective electronegativities or electron densities.[40]

Conventional CHF calculations, using large polarized basis sets, of ^{19}F shielding in PF_4^+, PF_3, PF_5, PF_6^-, SiF_4, and BF_3 have been reported.[11, 41, 42] The results are shown in Table 7.

Table 7. *^{19}F Shielding Calculated by Conventional CHF Method, ppm*

	Ref.	σ_{av}[a]	Expt	$\sigma_{\parallel}-\sigma_{\perp}$	Expt
SiF_4	41	363.9	363.2[b], 370.1[c], 371.1[d]	367.2	≈90[f]
BF_3	41	332.1	327.2[b], 327.4[e]	g	
PF_5 ax	42	293.5	} 266 (av)[h]	192	
PF_5 eq	42	300.4		172	
PF_3	11	269.5	228.3[b]	−12.5	−49
PF_4^+	11	314.5		166.2	
PF_6^-	11	319.1	260[h]	203.8	

[a] Gauge origin at center of mass; [b] σ_0 value, Ref. 43; [c] From σ^{SR} = −100.60 ppm[44] + σ^d(F atom) = 470.71 ppm[22]; [d] See Ref. 43; [e] From σ^{SR} = −143.3 ppm[44] + σ^d(F atom) = 470.71 ppm[22]; [f] From Ref. 45, $\Delta C = 2.2 \pm 1.9$ kHz, or from Ref. 46, $\Delta C \leq 3$ kHz, from which we calculate $\Delta\sigma^{SR} \approx 90 \pm 80$ ppm $\approx \Delta\sigma$; [g] σ_{xx} = 411.7 ppm, σ_{yy} = 206.6 ppm, σ_{zz} = 377.9 ppm, with z axis perpendicular to molecular plane and x axis along B–F bond; [h] Ref. 47.

In this review period several papers have appeared which report IGLO calculations of the ^{13}C shielding tensor elements in various compounds, comparisons of these with experiment, and the analyses of the individual MO contributions to the shielding which are standard output of IGLO calculations.[48-51] By rotating the shielding tensor from the molecular frame in which they are calculated, into a local bond frame in which one component is selected along the bond, the electronic structural basis of ^{13}C nuclear shielding can be studied. This is a technique which was used earlier for comparing ^{19}F shielding tensor elements in the CF_3X and CH_nF_{4-n} series o molecules, where X = H, F, Cl, Br, I.[52, 53] The rotated tensor elements parallel to the C–F bond, in the CFX plane and perpendicular to the CFX plane could then be compared directly in molecules of different symmetry. The ^{13}C shielding analyses went even further [48-51] By rotating the shielding tensor into a local bond

frame with one component along the bond, the explicit structural dependence of the contributions to the shielding are eliminated, thereby exposing detailed information on the dependence of the shielding tensor on the nature of each bond directly attached to the nucleus in question. Comparing "diamagnetic" and "paramagnetic" contributions from individual bonds directly attached to the ^{13}C reveals very useful qualitative trends, some of which would otherwise not have been noticed.

Since multiple local gauge origins are used when gauge factors are associated with each MO in the IGLO method, the partitioning into "diamagnetic" and "paramagnetic" terms, although well-defined in the context of the method, does not have a simple or known relationship with the diamagnetic and the paramagnetic parts of the shielding which are obtained when a unique gauge origin is used in the conventional CHF calculation. The practical advantage of local origin methods such as GIAO, IGLO, and LORG (These methods were discussed in the previous volume of this series.) lies in that they effectively leave out contributions which are of equal or nearly equal magnitude in both the conventional diamagnetic and paramagnetic parts, and in so doing lead to an effective damping of basis set errors resulting from use of a finite basis set. For example, "diamagnetic" terms for ^{13}C in IGLO calculations in CH_4, C_2H_6, $H_2C{=}CH_2$, $HC{\equiv}CH$, CH_3OH, CH_3NO_2, CH_3F, and CH_3SH,[49] and likewise for the methine carbon in isobutane, bicyclo[1.1.1] pentane, cubane, and tetrahedrane,[50] show contributions from C–C and C–H bonds which are almost spherically symmetric and also nearly constant, so that all of the chemical shift effects, as well as the shielding anisotropy, originate in the "paramagnetic" terms.[49] This is in sharp contrast with the anisotropic diamagnetic terms calculated using a unique origin. For example, the diamagnetic terms for C_1 in $H_2C{=}CH_2$, with origin at C_1, are 355.7 ppm, 340.6 ppm, 293.1 ppm for the xx, yy, zz components, respectively, with z axis along C=C and x axis perpendicular to the molecular plane.[33]

Some of the useful insights obtained from such analyses are cited below.

1. The β-methyl substituent effect can be associated with a consistent increase in the perpendicular component of the C–C bond contribution for the CH_3 groups for the series methane, ethane, propane, isobutane, and neopentane.[49]

2. All C–H and C–X bond contributions to methyl shielding indicate cylindrical symmetry of the electronic distribution along CX bonds.[51]

3. Different results have been found to be characteristic of strained bonds.[49] The observed high sensitivity to the CCC angle of the shielding component perpendicular to the ring, observed in the $^{13}CH_2$ shielding tensors of cycloalkanes,[54] comes from the intrinsic angular dependence that is characteristic of the C–C bonds themselves.

4. The substituent effect on the ^{13}C shielding, a downfield shift increasing with the electronegativity of X, is associated with the downfield shift of the perpendicular

component of the C–X "paramagnetic" bond contribution as the electronegativity of X increases.[49]

5. Aliphatic ^{13}C shielding tensors are sensitive to the molecular structure. In methine carbons the component parallel to the CH bond is determined almost completely by the C–C bond contributions, which depend on CCC angles.[50] The methyl shielding difference in *cis*- and *trans*-butene arises primarily from the upfield contribution from the *C–C bond in the *cis* compound compared to the *trans*. Additional contributions are also observed from the *C–H bonds. The remaining difference comes from the somewhat larger remote contributions in the *trans* than in the *cis* compound.[51] On the other hand, olefinic ^{13}C shielding tensors exhibit larger anisotropies but less variation with structure.[50]

6. A carbonyl substitution has a dramatic effect on the component parallel to the C–C* and in the O=C-C*H plane, owing to a large paramagnetic contribution involving the carbonyl π* LUMO.[50]

In summary, the symbiosis of experiment and theory in the assignment and analyses of the ^{13}C shielding tensor elements in relatively small molecules has proven to be very effective. The insight gained by analyzing the contributions to the shielding in these smaller molecules can later be very useful in the interpretation of ^{13}C shielding tensors in much larger systems.

C. Semi-empirical Calculations.— An empirical relationship for predicting chemical shifts of 12 different nuclei in 42 series of compounds containing any of 34 different alkyl substituents ranging from C_1 to C_{13} has been obtained.[55] The correlation equation is of the simple form

$$\delta(X) = m\sigma_a + b \qquad (12)$$

where σ_a is the substituent constant of an alkyl group and *m* and *b* are constants for a given series of compounds. The substituent constant σ_a for each alkyl group is calculated in a simple way entirely from bond refractions, R_D = 1.676 for C–H, 1.296 for C–C, according to the alkyl group geometry relative to the C–X bond. Data on more than 400 compounds were used, correlation coefficients in the fitting of *m* and *b* are better than 0.97 in nearly all series. The range of chemical shifts covered in each series is about 20 ppm for ^{13}C, 50 ppm for ^{15}N, 120 ppm for ^{17}O, 140 ppm for ^{19}F, 400 ppm for ^{77}Se, and 600 ppm for ^{199}Hg. No explanation was offered for the possible connection between bond refractions and contributions to nuclear shielding. In covalent molecules the molar refraction, $(4\pi/3)\ N_{Avo}\ \alpha_0$, is approximately the sum of bond refractions. That the chemical shift of a nucleus attached to an alkyl group is linearly related to some sum of bond contributions to the electric dipole polarizability of an alkane, with the parts adding up as projections of the bond refractions treated like vectors, is a bit surprising. It will be interesting to find out by IGLO calculations why this empirical correlation works. It may be that the analysis of bond contributions to shielding by the IGLO method will reveal the basis for this type of correlation.

Substituent chemical shifts (SCS) for ^{13}C in substituted adamantanes and norbornane have been calculated by the GIAO-FPT method at the INDO level.[56]

$$SCS = \sigma(C_\alpha, \text{parent}) - \sigma(C_\alpha, \text{derivative})$$

Some experimentally observed trends are reproduced by the calculated SCS values when the parametrization of the INDO method is modified. The α-SCS values correlate with the calculated local atomic charge at the carbon atom α to the site of substitution in the adamantanes and the norbornanes. The ^{13}C chemical shifts in 19 cyclic $4n\pi$ anion systems correlate with calculated local atomic charge according to the usual

$$\delta(\text{anion}) = \delta(\text{neutral}) - K(\rho_\pi - 1) \quad (13)$$

but with the parameter K determined as follows,[57]

$$K = 134 - 2.4(n/\rho_\pi)X_H \quad \text{ppm/e}^- \quad (14)$$

where n is the total number of carbon atoms in the system and X_H is a parameter obtained from the proton shift difference between the anion and the neutral. The term in X_H is interpreted as a magnetic anisotropy contribution to ^{13}C shifts such as that which is given by a ring current model. ^{19}F chemical shifts in a series of four perfluorinated annulenes, $C_nF_n^{\pm}$, $n = 3, 5, 6, 7$, correlate with the total electron density at F rather than the pi-electron density.[58] In perfluorinated linear aliphatic compounds, ^{19}F chemical shifts are modeled empirically, with terms including the influence of distant atoms (up to 5 bonds).[59]

The interpretation of shielding in d^6 transition-metal complexes[60] (reviewed earlier in this series, Vol. 15) which incorporates the nephelauxetic ratio, $\beta = B_{complex}/B_{gas}$, within the framework of the parametric d^q model is an improvement over the original $\sigma^p = -A/\Delta E$ model, taking into account other quantities which vary with the complex. Covalent bonding between metal and ligands is neglected.

The **L** matrix elements were calculated in terms of the empirical parameters Δ and B to allow for deviations from the strong-field limiting value of $8^{1/2}$ ħ. By plotting γ_M of the transition metal nucleus in several complexes against

$$\beta \sum_{\alpha=x,y,z} |\langle a^1A_{1g}|L_\alpha|a^1T_{1g(\alpha)}\rangle|^2/\Delta E\,(a^1T_{1g(\alpha)} - a^1A_{1g})$$

one obtains a good fit to a straight line, thereby obtaining the unknown parameter $\langle r_{3d}^{-3} \rangle / \beta$ from the slope and the value of $\gamma_0[1 - \sigma^d(\text{free M atom})]$ from the intercept. It appears that using the strong field limit for four d^6 complexes of Ru(II) is good enough[61] since the linear plot has an intercept which is the same as the value for the free Ru atom (obtained in an atomic beam measurement). $\langle r_{4d}^{-3} \rangle / \beta$ is 5.6 a.u., in agreement with the value for a 4d electron in the free ion.

This model for σ^p can also be used to correlate the chemical shifts of the ligand nuclei if the latter are assumed to be entirely due to the transition metal magnetic anisotropy.[62] A more appropriate approximate theory is that given by Buckingham

and Stephens,[63] which properly takes into account the M d electron wavefunctions at the ligand position, provided the theory can be corrected for covalency, which is not easily done except by a full CHF calculation such as for transition metal shielding by Nakatsuji et al.[64,65] At the semiempirical level the ligand shielding can be partitioned as follows

$$\sigma = \sigma(\text{free ligand}) + \sigma_{cov} + \sigma_M \quad (15)$$

where σ(free ligand) is the shielding in the unperturbed ligand, σ_{cov} represents corrections to the shielding due to the changes in the ligand orbitals associated with covalency of the metal–ligand bond, and σ_M are shielding contributions due to neighboring atoms, primarily the transition metal. The Buckingham-Stephens model calculates σ_M by using transition metal ion wavefunctions in the field of point charges. Bramley et al.[62] use McConnell and Pople's approximation[66, 67]

$$\sigma_M \cong (\chi_{zz} - \chi_{xx}) \langle 1-3\cos^2\theta \rangle /3R^3 \quad (16)$$

where $(\chi_{zz} - \chi_{xx})$ is the magnetic susceptibility anisotropy of the neighbor M, θ is the angle between the z axis and the vector R from the ligand nucleus to the neighbor M. Here χ_{zz} and χ_{xx} are taken to be the temperature-independent paramagnetism which are the logical counterparts of the σ_{zz}^p and σ_{xx}^p of the model, that is,

$$\sigma^p \cong -2 \langle r^{-3} \rangle \chi^p$$

where, in Bramley's model, $\langle r^{-3} \rangle$ is $\langle r_{3d\text{complex}}^{-3} \rangle /\beta$. $[Co(NH_3)_5Cl]^{2+}$ happens to have a very small anisotropy of L, i.e., the values of $\langle a^1A_{1g} \mid L_\alpha \mid a^1T_{1g} \rangle$ are 2.910, 2.902, and 2.902 for α = z, y, x, respectively. This would relate ligand shielding to

$$\approx \frac{\beta}{\Delta E(a^1T_{1g(z)} - a^1A_{1g})} - \frac{\beta}{\Delta E(a^1T_{1g(x)} - a^1A_{1g})}$$

Thus, in order to adequately represent the observed shielding of ^1H and ^{14}N in these complexes, the concept of anisotropic nephelauxetism has been introduced, i. e.,

$$\approx \frac{\beta_{(xy)}}{\Delta E(a^1T_{1g(z)} - a^1A_{1g})} - \frac{\beta_{(yz)}}{\Delta E(a^1T_{1g(x)} - a^1A_{1g})}$$

The z component of the transition $a^1A_{1g} \rightarrow a^1T_{1g}$ may be associated with the xy plane, and the x component with the yz plane. The $\beta_{(xy)} / \Delta E(a^1T_{1g}(z) - a^1A_{1g})$ term is a constant determined only by the properties of the central ion and the ammonia ligands in $[Co(NH_3)_5L]^{2+}$. The x terms which carry almost all the covalency influence of the L ligand upon the H and N shielding determine these shifts with change in L. In practice the term $\beta_{(yz)} / \Delta E(a^1T_{1g}(x) - a^1A_{1g})$ turns out to be monotonically related to the average $\beta/\Delta E$ of the pentaammine. Thus, the ^1H and the ^{14}N shifts follow the same chemical trend as the ^{59}Co shifts when the L ligand is varied. The neighbor magnetic anisotropy model for σ_M, being a long-range approximation, should be (and is) better for ^1H than for ^{15}N.

The ^{205}Tl chemical shifts in Tl(III) = [Xe] $4f^{14}5d^{10}$ compounds can be interpreted in a manner analogous to ^{63}Cu shifts in Cu(I) = [Ar]$3d^{10}$. The latter

have been calculated by Nakatsuji,[64] and the qualitative picture which arises from the orbital analysis of the ab initio results for σ in CuCl, $Cu(NH_3)_2^+$,$Cu(CN)_4^{3-}$, and $CuCl_4^{3-}$ is that there are two mechanisms. The d mechanism involves back-donation of electrons from the metal d orbitals to the ligands; the holes in the metal d orbitals contribute to σ^p. The p mechanism, less important in Cu(I), involves donation of electrons from the ligands to the metal p orbitals, which electrons contribute to σ^p. For the d mechanism the electron-withdrawing ligand leads to larger σ^p (less shielding). This appears to hold for Tl(III). On the other hand, in Tl(I) = $[Xe]4f^{14}5d^{10}6s^2$ the ^{205}Tl shielding increases with the electron-withdrawing ligand. For example,

$$\sigma(TlI) < \sigma(TlBr) < \sigma(TlCl) \quad .$$

The least-shielded ^{205}Tl in the TlI compound has the most p character, which comes with increased mixing of 6s and 6p.[68]

2 Physical Aspects of Nuclear Shielding

A. Anisotropy of the Shielding Tensor.— The usual conventions are used here for shielding components, that is, $\sigma_{//}$ corresponds to the component along the symmetry axis, so that the anisotropy of axial systems is $\sigma_{//} - \sigma_\perp$ and can be of either sign. $\Delta\sigma_{33} = \sigma_{33} - \sigma(ref)$ and chemical shifts $\delta = \sigma(ref) - \sigma$, with positive δ at higher frequency compared to the reference nucleus. The numbering system for the principal axes is such that $\sigma_{33} \geq \sigma_{22} \geq \sigma_{11}$, that is, the 33 component corresponds to the lowest frequency, or $\delta_{33} < \delta_{22} < \delta_{11}$. Some authors still use the Haeberlen convention, $|\sigma_{33} - \sigma_{iso}| > |\sigma_{11} - \sigma_{iso}| \geq |\sigma_{22} - \sigma_{iso}|$, not used here. Unfortunately, some authors use the symbol σ when they really mean δ.

The ^{207}Pb shielding tensor in *tetra-p*-tolyl-lead is axially symmetric,

$$\delta_{//} = \sigma(ref) - \sigma_{//} = -43 \text{ ppm}$$
$$\delta_\perp = \sigma(ref) - \sigma_\perp = -181 \text{ ppm}$$

where ref = $PbMe_4$, 70% solution in toluene. Solution-to-solid shifts are modest (about 40 ppm). ^{207}Pb in *hexa-p*-tolyldilead exhibits pronounced axial or nearly axial shielding anisotropy at both Pb sites.[69]

^{195}Pt shielding tensors in several environments have been reported (see Table 8).[70]

The ^{183}W shielding tensor has been measured in phosphotungstic acid, $H_3[P(W_{12}O_{40})] \cdot nH_2O$: $(\Delta\sigma_{11}, \Delta\sigma_{22}, \Delta\sigma_{33}) = -409, -148, +1079$ ppm, where $\Delta\sigma_{11}$ is $\sigma_{11} - \sigma(Na_2WO_4$, satd. soln.) There are 12 equivalent W atoms, each octahedrally coordinated by oxygen atoms, forming a cage with the phosphorus site at its center. ^{183}W in $CaWO_4$ shows a small shielding anisotropy and in $W(CO)_6$ is isotropic as expected.[71]

The ^{125}Te shielding tensor in tellurophene (C_4H_4Te) dissolved in a liquid

crystal is characterized by $\sigma_{xx} - \sigma_{yy} = 307 \pm 26$ ppm and $\sigma_{zz} - (1/2)(\sigma_{xx} + \sigma_{yy}) = -1569 \pm 21$ ppm.[72] The isotropic shielding is also reported as σ_{iso}(in l.c.) – $\sigma(Me_2Tl$ liq.) ≅ 35 ppm. (There are minor differences, 2 ppm at most, in different liquid-crystal solvents.) This leads to

$$\Delta\sigma_{zz} = -1011 \text{ ppm}, \Delta\sigma_{xx} = 711.5 \text{ ppm, and } \Delta\sigma_{yy} = 404.5 \text{ ppm}$$

(the standard reference being liquid Me_2Te), in which z is along the molecular symmetry axis and y is perpendicular to the molecular plane. The least shielded component is along the symmetry axis. The principal axes of the ^{113}Cd shielding tensor in $Cd(OAc)_2 \cdot 2H_2O$ have been unambiguously assigned,[73] confirming the earlier assignment,[74] which was based on symmetry arguments and empirical rules previously used in semiempirical interpretation of Cd shielding tensor elements in a variety of environments. The ^{57}Fe shielding anisotropy $|\sigma_{//} - \sigma_{\perp}| = 7630$ ppm was obtained from relaxation measurements in ferrocytochrome c, for which $\sigma_{iso} - \sigma(Fe(CO)_5) = -11200$ ppm.[75] In this protein the ^{57}Fe nucleus is in a porphyrin complex. The suggested assignment is

$$\sigma_{\perp} - \sigma(Fe(CO)_5) = -8650 \text{ ppm and}$$
$$\sigma_{//} - \sigma(Fe(CO)_5) = -16280 \text{ ppm,}$$

based on comparison with other ^{57}Fe porphyrin chemical shifts, that is,

$$\sigma_{//} - \sigma_{\perp} = -7630 \text{ ppm.}$$

Table 8. *^{195}Pt Shielding Tensors, ppm*[70]

^{195}Pt in	$\Delta\sigma_{33}$[a]	$\Delta\sigma_{22}$	$\Delta\sigma_{11}$	$\Delta\sigma_{iso}$	$(\sigma_{solid} - \sigma_{soln})$
$K_2[Pt(OH)_6]$	–3218	–3567	–3643	–3476	–186
cis-$[PtMe_2(PEt_3)_2]$	5058	4649	4256	4654	~0
$[Pt(en)_3]Cl_4 \cdot 2H_2O$	1174	1070	585	943	
cis-$[PtCl_4(NH_3)_2]$	367	209	134	237	92
$Na_2[PtCl_6] \cdot 6H_2O$	–85	–85	–85	–85	–85

[a] $\Delta\sigma_{33}$ is defined as $\sigma_{33} - \sigma$ ($[PtCl_6]^{2-}$ in D_2O).

The ^{31}P shielding tensor elements in monofluorophosphates were obtained by broadline and MAS NMR spectroscopy.[76] $\sigma_{//} - \sigma_{\perp} = -142$ ppm, $\sigma_{iso} - \sigma(H_3PO_4$ std ref) = –5.9 and +2.4, respectively, in Na_2PO_3F and $BaPO_3F$. In $K_2P_2O_5F_2$ the two PO_3F tetrahedra are connected via a bridging oxygen. The two ^{31}P nuclei are not equivalent but have very similar shielding tensors since each P has one bridging oxygen, one F, and two terminal oxygens attached to it. $\sigma_{iso} - \sigma(H_3PO_4$ std ref) = +29.4 ± 3 and +26.4 ± 3 ppm. The ^{31}P in the $P_2O_5F_2^{2-}$ moiety is compared to the ^{31}P in the phosphate middle group $-O_B-P(O_T)_2-O_B-$ in condensed phosphates. ^{31}P shielding tensors have been reported in ortho-, pyro-, poly-, and metaphosphates.[77-79] The sign of the shielding anisotropy provides a definitive assignment of the nature of phosphorus coordination in these axial or nearly axial environments, i.e., of

differentiating end ($\sigma_{//} - \sigma_{\perp} < 0$) and middle ($\sigma_{//} - \sigma_{\perp} > 0$) units. Furthermore, the level of protonation, hydration state, counter ions, crystalline form, and solid state molecular distortions affect the individual tensor components. Terminal groups have an approximate three-fold axis of local symmetry, but in some cases some deviation from axial symmetry is shown by asymmetry parameters 0.22 – 0.44. NMR thus reveals structural inequivalences more readily than x-ray data. The isotropic shieldings show a linear correlation with various quantities such as electronegativity, $Z / \sqrt{r}$ (cation charge, cation radius)[78, 80] and the anisotropy shows a direct proportionality to the average deviation of the O–P–O angle from tetrahedral.[78]

The anisotropies of the ^{1}H, ^{13}C, and ^{19}F shieldings in CH_3F have been measured in nematic liquid crystals.[81] The anisotropy, $\Delta\sigma(^{19}F) = -90 \pm 4$ ppm, is somewhat larger than the – 60.8 ppm experimental value from molecular beam data[44] and the –71.5 ppm theoretical value from GIAO-FPT calculations.[82] It is expected that the effect of the liquid crystal on the shielding anisotropies is somewhat larger than the 2% estimated. The reported anisotropy of the proton shielding, $\Delta\sigma = \sigma_{zz} - \frac{1}{2}(\sigma_{xx} + \sigma_{yy}) = 5.2 \pm 0.2$ ppm (z is along the C–H bond) is close to the theoretical result: $\Delta\sigma = 4.51$ ppm,[83] although the value of $\Delta\sigma = -3.6$ ppm was also measured in a smectic phase. On the other hand, the ^{13}C shielding anisotropy, 87.4 ± 3.5 ppm is very close to that obtained by Zilm et al. for CH_3F in solid Ar, ($\Delta\sigma = 90$ ppm)[84] and the theoretical calculations ($\Delta\sigma = 85.9$ ppm[82] or 86.9 ppm[85]). The F and the H nuclei, being peripheral nuclei, suffer larger medium effects than the ^{13}C nucleus in CH_3F. In CH_3PCl_2 in nematic mixed liquid crystals $\Delta\sigma(^{1}H) = -11.0 \pm 0.1$ ppm.[86]

^{13}C shielding tensors in a variety of molecules have been obtained at 20 K in an inert gas matrix, in a continuing study by D. M. Grant and coworkers.[48, 50, 51] Methyl carbons in 18 molecules (methoxy methyls, methyls in alkanes, alcohols, and ketones, methyls attached to sulfur, and in *cis*- and *trans*-butene) have been analyzed; principal axes are assigned and theoretical local-bond contributions are presented.[51] The σ_{33} axes deviate from the local C_3 symmetry axis of the CH_3 group by up to 15 degrees. Methine carbons in $(CH_3)_3CH$, $(CH_3O)_3CH$, bicyclo[1.1.1] pentane, bicyclo[1.1.1]pentanone, norbornadiene, cubane, and tetrahedrane have ^{13}C shielding tensors which are highly sensitive to the electronic structure of the molecule.[50] A review of the ^{13}C shielding tensors and the local bond analyses thereof provides a summary of the types of information, some obvious, some rather subtle, which are emerging from this method.[48]

The ^{13}C shielding tensors in a single crystal of pyrene have been determined.[87] The orientations of the principal axes are shown in the figure: the dashed lines are σ_{11}, while dotted lines are σ_{22} and all σ_{33} are perpendicular to the molecular plane. Values are shown in Table 9 for the unique carbons. All others are related by symmetry.

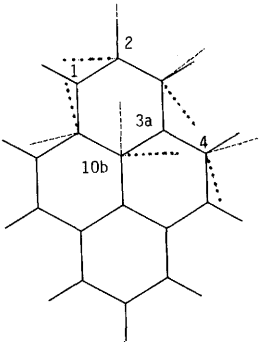

Table 9. *^{13}C Shielding Tensors in Pyrene, ppm*[87]

	$\sigma_{11} - \sigma$(TMS)	$\sigma_{22} - \sigma$(TMS)	$\sigma_{33} - \sigma$(TMS)
C_1[a]	−212	−141	−21
C_2	−226	−140	−4
C_4	−222	−136	−21
C_{3a}	−213	−187	+7
C_{10b}	−197	−191	+18

[a] See figure above for numbering of carbons.

When the mean excitation energy approximation is used for ^{13}C shielding calculations in a molecule like pyrene, the paramagnetic term can be expressed in terms of bond orders.[67, 88] The correlation of the in-plane shielding tensor components with bond orders P_{AB} calculated by MNDO reveals the following general trends which can be used to assign ^{13}C shielding tensor components in other fused-ring aromatic systems. The magnitude of the paramagnetic term is greatest for the least- shielded (highest frequency) component, σ_{11} in the usual convention. Thus, general trends in σ_{11} are observed: σ_{11} tends to lie along the bond with the smallest P_{AB} or perpendicular to the bond of largest P_{AB}. When two of the three bond orders are equal, σ_{11} lies along the unique bond when its bond order is the smallest, or perpendicular to the unique bond when its bond order is the largest. For the case where all three bonds exhibit different bond orders, then the σ_{11} axis strikes a compromise between being parallel to the bond with the lowest bond order and perpendicular to the bond with the highest bond order. The magnitudes of both σ_{11} and σ_{22} show a very good ($r = 0.9914$) linear correlation with the calculated paramagnetic term, implying that both in-plane components have nearly the same diamagnetic parts for all carbons in the molecule. By Flygare's model,[18] this is just

$$\sigma^d_{\alpha\alpha} \cong \sigma^d(\text{free atom}) + \left(\frac{\mu_0}{4\pi}\right) \cdot \frac{e^2}{2m} \sum_N{}' Z_N \left(\frac{R_\beta^2 + R_\gamma^2}{R^3}\right)_N \quad . \tag{18}$$

For one in-plane axis α, there are contributions only from R_β^2, the distances of other

nuclei along the other in-plane axis, so that σ_{11}^{d} and σ_{22}^{d} in benzene, for example, are nearly equal,[89] unlike σ_{33}, in which two in-plane distances are involved in a much large σ^{d}. The large positive shielding component perpendicular to the molecular plane is characteristic of planar aromatic molecules and has been found in benzene to be due primarily to local diamagnetic circulations around carbon atoms and currents localized around the C–C bonds, rather than the pi electrons.[89]

The ^{13}C shielding tensor of the carbonyl carbon of dimethyloxalate, a model for carbonyl groups in ester-linked fatty acids, has been shown by single-crystal study to be similar to other carbonyl environments, that is, σ_{22}[90] is along the C=O bond, σ_{11} is in the molecular plane, and σ_{33} is perpendicular to the molecular plane.

B. Effects of Vibration and Rotation. — Nafie and Freedman[91] introduced the concept of a vibrational magnetic shielding tensor with components $\sigma_{\alpha\beta}^{vib}$ for a vibrating molecule in an external magnetic field B_β. This tensor gives rise to an effective magnetic field at nucleus I equal to $-\sigma_{\alpha\beta}^{vib}B_\beta$. This is a vibrational contribution to shielding which comes about because the vibrational nuclear angular momentum generates an electronic angular momentum. For nucleus I, Nafie and Freedman derived the following,

$$\sigma_{\alpha\beta}^{vib} = -\frac{2ie^2\hbar}{m}\varepsilon_{\alpha\mu\lambda}\sum_{n\neq 0}\frac{\langle 0|\sum_i (r_{i\lambda}-R_\lambda)\, r_{ile}^{-3}|n\rangle\langle n|\sum_i \mathfrak{L}_{i\beta}|0\rangle}{R_{\mu e}(E_n-E_0)^2} \qquad (19)$$

where α, β, μ, λ = x or y or z, $\mathbf{r}_i$ is the position vector of electron i, $\mathbf{R}$ is the position of nucleus I, $\mathbf{R}_e$ at the equilibrium nuclear position, and r_{ile} is the distance of the ith electron from nucleus I at the equilibrium nuclear position. $|0\rangle$ and $|n\rangle$, with corresponding energies E_0 and E_n, are the solutions of the electronic hamiltonian at the equilibrium nuclear positions. $\mathfrak{L}_i$ is the angular momentum operator of the ith electron and $\varepsilon_{\alpha\mu\lambda}$ is the coefficient which relates the angular momentum operator to position and linear momentum, as in

$$\mathfrak{L}_{i\alpha} = \varepsilon_{\alpha\mu\lambda}\, r_{i\mu}\, p_{i\lambda} \quad . \qquad (20)$$

Alternatively, the vibrational shielding tensor may be written in terms of derivatives of the ground-state wavefunction:

$$\sigma_{\alpha\beta}^{vib} = \frac{2i\hbar}{R_{\mu\varepsilon}Ze}\,\varepsilon_{\alpha\mu\lambda}\langle(\partial\psi_0/\partial R_\alpha)_e|(\partial\psi_0/(\partial B_\beta)_e\rangle \qquad (21)$$

in which Ψ_0 is the ground state solution of the electronic hamiltonian in the presence of the perturbing field, which electronic wavefunction contains a description of the adiabatic following of electronic charge density with nuclear positions (and adiabatic following of electronic current density with nuclear momenta). Ze is the nuclear charge. Since $\sigma_{\alpha\beta}^{vib}$ depends on the vibrational nuclear angular momentum, it should provide a contribution to nuclear magnetic shielding when the molecule is in a

degenerate vibrational state. The magnitude of this contribution is relatively small, as is evident in $(E_n - E_0)^{-2}$ in Equation (21), compared to $(E_n - E_0)^{-1}$ in the usual paramagnetic term. The physical picture presented by Nafie and Freedman makes this clear. Whereas the paramagnetic term of the shielding depends on the intrinsic nuclear magnetic moment and the steady-state electronic angular momenta set in motion by the applied magnetic field, this vibrational magnetic shielding depends on the nuclear angular momenta and nuclear-generated electronic angular momenta, both of which oscillate about a value of zero angular momentum as the molecule undergoes vibrational motion. This provides a contribution which explicitly depends on nuclear coordinates, whereas the usual diamagnetic and paramagnetic terms in shielding implicitly depend on nuclear coordinates. All contributions averaged over the nuclear wavefunctions give rise to the nuclear shielding characteristic of each rovibrational state of the molecule. The observed nuclear shielding is a population-weighted average of such quantities, which weighting depends on masses and temperature, giving rise to the familiar isotope shifts and temperature dependent chemical shifts. Calculations of isotope shifts and temperature-dependent chemical shifts have included only the diamagnetic and the paramagnetic shielding and have been made in the context of the Born-Oppenheimer (BO) approximation.[92] This new term is a much smaller contribution, which is non-BO in origin. Although the latter is entirely responsible for VCD intensities, it appears to be too small to be important in dynamic averages of NMR chemical shifts.

Theoretical interpretation of isotope shifts and temperature-dependent chemical shifts has been reviewed in previous volumes. In the BO context each term which contributes to these shifts involves an electronic factor like $(\partial\sigma/\partial\Delta r)_e$, which describes the change in the nuclear shielding upon a change in the length of a bond involving that nucleus (primary) or a remote bond (secondary), and a dynamic factor which is a displacement coordinate averaged over the nuclear motions. For temperature-dependent shifts, the latter is a difference of thermal average bond lengths or angles at different temperatures. For isotope shifts the latter is a difference of thermal averages for different isotopomers. Theoretical calculations of the electronic factors for hydrides of first- and second-row elements have been reported by Chesnut.[93] There are several important findings. Previous calculations have revealed negative values of primary derivatives $(\partial\sigma_M/\partial\Delta r_{MX})_e$ in every case except for ^{7}Li in LiH, which has been found positive by several methods of calculation.[94-96] Negative values of $(\partial\sigma/\partial\Delta r)_e$ translate to negative isotope shifts (heavier isotopomers appear at lower frequency) since the dynamic factors are invariably of the same sign $[\langle\Delta r\rangle_{heavy} - \langle\Delta r\rangle_{light} < 0]$. Although the isotope shift for ^{7}Li in LiH/LiD has not been observed, there is little doubt that the sign will be unusual, owing to the unusual sign of $(\partial\sigma_{Li}/\partial\Delta r_{LiH})_e$. It is of interest, therefore, to find out whether this is a singular phenomenon or part of a smooth trend. The Chesnut calculations show the latter (see Figure 1)[93].

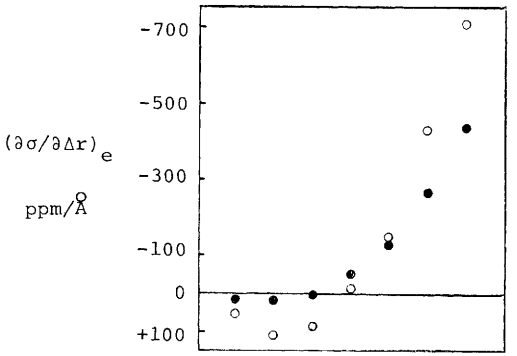

Fig. 1 Variation of $(\partial\sigma/\partial\Delta r)_e$ with column of periodic table of the heavy atom for the first row(●) and second row (○) hydrides.[93]

Although these calculations are for hydrides only, generalization to other systems will soon become available. If these trends can be expected in other systems as well, then Figure 1 explains why most one-bond isotope shifts are negative. The positive derivatives occur for nuclei which are in the first three groups, alkali, alkaline earths, and the boron family, but the great collection of reported isotope shifts are for the nuclei in groups 4-7. The presence of a net charge on the system affects the derivatives in a regular algebraic way, a net negative charge makes the values more negative, a net positive charge makes the values more positive. Thus, $(\partial\sigma/\partial\Delta r)_e$ for NH_3, NH_4^+ are -130.3, -67.9 ppm $Å^{-1}$, for PH_3, PH_4^+ are -150.8, -52.9 ppm $Å^{-1}$. Also, $(\partial\sigma/\partial\Delta r)_e$ for BH_3, BH_4^- are $+3.5$, -27.0 ppm $Å^{-1}$; for AlH_3, AlH_4^-, they are $+84.2$, $+11.6$ ppm $Å^{-1}$.[93]

The ^1H shielding in these hydrides (except for diatomic molecules) depend on two derivatives, primary $(\partial\sigma_{H_1}/(\partial\Delta r_{MH_1})_e$ and secondary $(\partial\sigma_{H_1}/(\partial\Delta r_{MH_2})_e$. The relative magnitudes of these derivatives have been predicted earlier[97] to be | primary| >> |secondary| usually. This general trend has been verified by the Chesnut calculations. In most cases (except for SiH_4) the primary is about one order of magnitude greater than the secondary. However, the latter has been predicted to be important for 2-bond isotope shifts in these molecules, and in general, secondary derivatives have been implicated in long-range isotope shifts.[98, 99] The calculations verify that the paramagnetic term dominates the shielding derivative with bond extension. It is in fact the derivative of the paramagnetic term that controls both the magnitude and the sign of the shielding derivatives. These do not parallel the paramagnetic term itself, rather, the relative sensitivity of the paramagnetic term to changes in bond length which is responsible for the variation across the periodic table seen in Fig. 1.[93] The relative sensitivity of the paramagnetic term to bond extension

has been discussed previously.[52, 100]

Much heavier molecules, SeF_6, TeF_6, and WF_6, $[V(CO)_6]^-$ and $[Co(CN)_6]^{3-}$, were the subject of other work.[99, 101-103] The ^{19}F, ^{77}Se, and ^{125}Te chemical shifts in the SeF_6, TeF_6, and WF_6 gas in the zero-pressure limit have been determined as a function of temperature.[101] The temperature coefficients of ^{19}F shielding in these molecules and in other binary fluorides correlate with the paramagnetic shielding term much better than with the absolute shielding. The dynamic averages such as $\langle \Delta r \rangle$, $\langle (\Delta r)^2 \rangle$ were calculated for all isotopomers of the MF_6 molecules for 200-400 K.[102] These were used in the interpretation of the observed temperature dependence of the ^{19}F shielding in the molecules SeF_6, TeF_6, and WF_6 in the zero-pressure limit and the isotope shifts.[102] The dynamic factors vary strictly linearly with $(m' - m)/m'$ in $^{m'}SeF_6$ compared to $^{m}SeF_6$ for $m' = 82, 80, 78, 77, 76, 74$, where m was chosen to be 74. A similar linear relation was found for $^{m'}TeF_6$ compared to $^{m}TeF_6$, where $m = 125$ and $m' = 125, 126, 128, 130, 132$. The temperature dependence of $\langle \Delta r \rangle$ has nearly the same curvature as the temperature dependence of the ^{19}F shielding in these molecules, which makes it possible to fit the latter by some combination of $\langle \Delta r \rangle$ and $\langle (\Delta r)^2 \rangle$; the electronic factors multiplying them are then empirically determined. Since the dynamic factors change with temperature in the same monotonic way, it is not practically possible to independently determine both $(\partial\sigma/\partial\Delta r)_e$ and $(\partial^2\sigma/\partial(\Delta r)^2)_e$. Rather, only an empirical parameter related to both can be extracted. This study therefore shows that the empirical parameter "$(\partial\sigma/\partial\Delta r)_e$" obtained by fitting to $\langle \Delta r \rangle^T$ actually includes $(\partial^2\sigma/\partial(\Delta r)^2)_e$, but the different curves which result from using different ratios of second to first derivatives of shielding cannot be distinguished in comparison with the experimental curves. By using Stanton and Bartell's force field to calculate the dynamic averages $\langle \Delta r \rangle$ and $\langle (\Delta r)^2$ in SF_6, an empirical parameter $(\partial\sigma/\partial\Delta r)_e = -1930$ ppm $Å^{-1}$ for ^{19}F in SF_6 is obtained from fitting to the temperature dependence and -2040 ppm $Å^{-1}$ from fitting the isotope shift. Alternatively, a best fit to both can be obtained with $(\partial\sigma/\partial\Delta r)_e = -1890$ ppm $Å^{-1}$ and $(\partial^2\sigma/\partial(\Delta r)^2)_e = -560$ ppm $Å^{-2}$.[102]

In the SF_6, SeF_6, TeF_6 series, ^{19}F shielding derivatives have no clear trend, -1930, -2690, -1770 ppm $Å^{-1}$ based on the temperature dependence. The ^{77}Se and the ^{125}Te empirical shielding derivatives are -1500 and -1050 ppm $Å^{-1}$.

The temperature dependence of the ^{51}V chemical shift in 14 vanadium complexes in solution have been measured.[99] ^{19}F chemical shifts in the liquid-phase are in the direction of decreasing resonance frequency with increasing temperature, due to the decreasing intermolecular effects accompanying expansion of the liquid.[104, 105] ^{51}V chemical shifts, on the other hand, show a shift to increasing resonance frequency with increasing temperature. This behavior is similar to ^{19}F shifts in the zero-pressure limit, in which the resonance frequency increases with increasing M–F bond extension. This behavior is similar to ^{59}Co in complexes in

solution and is believed to be true in general for transition metal shielding in complexes. The intermolecular effects may be just as large as for ^{19}F, but they are negligible compared to the very large shifts which attend increasing transition metal-ligand distance. Thus, it is possible to obtain $\sigma_0(T)$ directly from condensed-phase temperature dependent shifts without going to the limit of the isolated molecule. These are large; $d\sigma_0/dT \cong -0.3$ to -1.5 ppm/deg have been observed. This is fortunate because the change of transition metal shielding with metal-ligand distance is of considerable interest. The vibrational analyses of $[V(CO)_6]^-$ and $[Co(CN)_6]^{3-}$ have been reported.[103] Using the dynamic averages $\langle\Delta r\rangle$ and $\langle(\Delta r)^2\rangle$ for the V–C, C–O, Co–C, and C–N bonds, it is possible to interpret the temperature-dependent ^{51}V and ^{59}Co shifts, as well as all the isotope shifts in $[V(CO)_6]^-$ and $[Co(CN)_6]^{3-}$ using the same theory as for other molecules previously studied. (A theory which had been proposed specifically for interpretation of ^{59}Co shifts in solution by Benedek et al.[106] is shown to have inconsistencies with known experimental trends in isotope shifts.) The obtained derivatives are large, $(\partial\sigma^V/\partial\Delta r_{VC})_e \cong -2\times 10^3$ ppm Å^{-1} in $[V(CO)_6]^-$ and $(\partial\sigma^{Co}/\partial\Delta r_{CoC})_e \cong -8\times 10^3$ ppm Å^{-1} in $[Co(CN)_6]^{3-}$, but these are entirely reasonable values when considered in terms of the chemical shift ranges for these nuclei. The temperature coefficients of the ^{51}V chemical shifts correlate in the same way with ^{51}V chemical shifts, as does ^{19}F temperature coefficients with only the paramagnetic part of ^{19}F shifts. This is not surprising. It is well-known that transition metal shifts are largely dominated by the changes in the paramagnetic term. This correlation can be interpreted qualitatively with the d^q model of transition metal shielding.[60] Starting with the Bramley et al. equation

$$\sigma^p = \text{constants}\times\beta\frac{|\langle a\,^1A_{1g}|L_z|a\,^1T_{1g}\rangle|^2}{\Delta E(a\,^1T_{1g}-a\,^1A_{1g})} \tag{22}$$

it is shown that

$$\left(\frac{\partial\sigma^p}{\partial r}\right)_e \cong \frac{c}{r_e}\sigma_e^p \quad\text{and}\quad \left(\frac{\partial^2\sigma^p}{\partial r^2}\right)_e \cong \frac{c-1}{r_e}\left(\frac{\partial\sigma^p}{\partial r}\right)_e \tag{23}$$

where c has a value between 5 and 6. According to theory, the temperature coefficients of ^{51}V shielding contain the electronic factor $(\partial\sigma^p/\partial r)_e$. The correlation will be observed if the dynamic factors $\langle\Delta r\rangle^T - \langle\Delta r\rangle^{300}$ are not widely different from one vanadium complex to another, and if as the d^q model predicts, $(\partial\sigma^p/\partial r)_e \propto \sigma_e^p$. The observed correlation of the temperature coefficients of ^{51}V shielding with vanadium chemical shifts is therefore consistent with the d^q model. Nevertheless, it appears that the limit of zero σ^p cannot be determined by extrapolation of that correlation to zero temperature coefficient. In the limit of very low temperature coefficients of $\sigma_0(T)$, which would accompany negligibly small σ^p, the intermolecular contributions to $(d\sigma/dT)$ can no longer be neglected.

An interesting comparison can be made using ^{17}O in a solution of UO_2^+ ion in H_2O. Both ^{17}O signals show linear frequency shifts with temperature, but the temperature coefficients are of opposite sign: ^{17}O in UO_2^+ shows typical $(d\sigma_0/dT) < 0$ behavior, i.e., shifts to higher resonance frequency at higher temperature, just as ^{51}V in $[V(CO)_6]^-$. On the other hand, ^{17}O in H_2O in the same sample shows the typical deshielding intermolecular effects which become less important at higher temperatures, that is, ^{17}O shifts to lower frequency at higher temperature.[107] The temperature coefficient of ^{17}O in UO_2^+ is not easily related to the observed 2-bond $^{18/16}O$-induced ^{17}O shift since the latter is related to and may even be dominated by the change in shielding of the ^{17}O due to the extension of the *other* U–O bond.

C. Isotope Shifts. — As in previous volumes, we use the convention that the isotope shift is given by

$$^{n}\Delta X(m'/mA) = \sigma(X \text{ in } {}^{m}A\text{-isotopomer}) - \sigma(X \text{ in } {}^{m'}A\text{-isotopomer}) = \delta(\text{heavy}) - \delta(\text{light})$$

for isotopic mass m'>m, so that the isotope shift is negative (usual sign) when the heavy isotopomer appears at lower frequency. The additivity of isotope shifts upon multiple substitution will no longer be commented upon since there have been few exceptions.

In $[V(CO)_6]^-$ and in $CpV(CO)_4$ the ^{51}V isotope shifts are $^{1}\Delta^{51}V(^{13/12}C) = -0.27$ ppm per ^{13}C and -0.46 ppm per ^{13}C, respectively. Also, $^{2}\Delta^{51}V(^{18/16}O) = -0.10$ ppm per ^{18}O for both $[V(CO)_6]^-$ and $CpV(CO)_4$.[108] These values and those of $^{1}\Delta^{59}Co(^{13/12}C)$ and $^{2}\Delta^{59}Co(^{15/14}N)$ in $[Co(CN)_6]^{3-}$ and $^{2}\Delta^{59}Co(^{2/1}H)$ in $[Co(NH_3)_6]^{3+}$ have been interpreted using the same theory as for the temperature shifts.[99] It is found that the temperature coefficient of ^{51}V shielding and the ^{51}V isotope shifts in $[V(CO)_6]^-$ are consistent with a derivative $(\partial\sigma^V/\partial\Delta r_{VC})_e \cong -2\times10^3$ ppm Å^{-1}. The very large isotope shift $^{1}\Delta^{51}V(^{2/1}H) = -4.7$ ppm in $[CpV(CO)_3H]^-$ is consistent with the large mass factors associated with deuteration,[108] which make this isotope shift very large compared to the shift upon ^{13}CO substitution.

In fluorinated biphenyls $^{n}\Delta^{19}F(^{13/12}C)$ drops off with increasing number of bonds n. Because of the dual paths connecting the ^{13}C to the ^{19}F, the observed isotope shifts may be considered as combinations $^{n}\Delta \pm {}^{(9-n)}\Delta$. Observed are $^{1}\Delta \pm {}^{8}\Delta = -82$ to -87 ppb, $^{2}\Delta \pm {}^{7}\Delta = -22$ to -27 ppb, $^{3}\Delta \pm {}^{6}\Delta = -3.5$ to -5.5 ppb and $^{4}\Delta \pm {}^{5}\Delta = -1.7$ to -2.5 ppb.[109] $^{n}\Delta^{19}F(^{13/12}C)$ in *para*-difluorobenzene are comparable to these. Here $^{1}\Delta = -90$ ppb, $^{2}\Delta \pm {}^{6}\Delta = -26$ ppb, $^{3}\Delta \pm {}^{5}\Delta = -5$ ppb, $2\,{}^{4}\Delta = -5$ ppb.[110] These ^{13}C-induced ^{19}F shifts in fluorinated benzenes and biphenyls are typical in magnitude. Long-range (7-8 bonds) ^{19}F isotope shifts in 4-fluorophenyl systems X–  –F upon deuteration in the X group were reviewed *in this series, Vol. 16, Chapter 1, in which please note a systematic error in Table 4, where* $^{7}\Delta^{19}F$ *signs should all be reversed.* Further work in the cations, X being –  , show that while β-deuteration leads to $^{7}\Delta^{19}F$ of unusual sign (+), i.e.,

shift downfield to higher frequency on deuteration as in the *corrected* Table, γ-deuteration leads to $^{8}\Delta^{19}F(^{2/1}H)$ of the usual sign (–). That is, an alternation of sign of the ^{19}F isotope shift on D-substitution in the alkyl cation tail of the fluorophenyl system. The magnitudes also are smaller (–14 to – 20 ppb per D for γ substitution,[111] compared to – 30 to – 154 ppb per D for β substitution.[111, 112] $^{1}\Delta^{19}F(^{m'/m}Se)$ and $^{1}\Delta^{19}F(^{m'/m}Te)$ have been measured for all naturally occuring isotopic masses of Se and Te in SeF_6 and TeF_6.[101] The isotope shifts exhibit the proportionality to (m' – 74)/m' and (m' – 125)/m', respectively, as predicted by theory.[113] Rovibrational calculations on SeF_6 and TeF_6 show that $\langle\Delta r\rangle_{m'} - \langle\Delta r\rangle_{m}$ does indeed exhibit proportionality to these mass factors.[102]

Deuterium isotope effects on ^{17}O chemical shifts in common NMR solvents (the usual sign) are given in Table 10.

Table 10. *$^{n}\Delta^{17}O(^{2/1}H)$, ppm per D*[114]

	$^{1}\Delta$	$^{2}\Delta$	$^{3}\Delta$	$^{2}\Delta + 6\,^{4}\Delta$
H_2O	–1.45			
CH_3OH	– 1.6			
CH_3OD		– 0.4		
$(CH_3)_2C{=}O$			+ 0.2	
$(CH_3)_2S{=}O$			– 0.13	
$(CH_3)_2N\text{-}CHO$				– 2.0

The value for liquid H_2O compares well with –1.54 ppm per D from earlier work,[115] and contrasts with – 2.02 ppm per D reported for the gas phase.[116] The unusual sign of the $^{3}\Delta^{17}O(^{2/1}H)$ in acetone parallels that of the $^{2}\Delta^{13}CO(^{2/1}H)$ in acetone, which is + 0.054 ppm per D [and parallels the unusual sign of the latter isotope shift in various CH_3COX molecules (see this series, Vol. 16, Chapter 1)]. We have suggested that $(\partial\sigma^{C(O)}/\partial\Delta r_{CH})_e$ is positive in $(CH_3)_3CO$ [and in CH_3COX]. It now appears that the ^{17}O shielding derivative $(\partial\sigma^{O}/\partial\Delta r_{CH})_e$ may also be positive in this molecule and 3.7 times larger than the ^{13}C shielding derivative. This factor is consistent with the known chemical shift ranges of ^{17}O vs ^{13}C.

The linear correlation of isotope shifts with the chemical shifts of the observed nucleus in a series of closely related molecules which has been predicted and observed in earlier work, e.g., $^{1}\Delta^{19}F(^{13/12}C)$ in fluoromethanes,[52, 117] and $^{1}\Delta^{13}C(^{18/16}O)$ for CO in acetophenones[118] has also been reported recently in $^{2}\Delta^{13}C(^{2/1}H)$ for sp^2 carbons in $CH_3CR{=}X$.[119] In all of these correlations the slope is positive, that is, increasing magnitude of isotope shifts with increasing resonance frequencies of the observed nucleus. A model based on hyperconjugation is advanced for the observed correlation in the $CH_3CR{=}X$ case,[119] but it is unnecessary to invoke a new mechanism which applies to this specific case but has no relevance to any of the other cases in which the same linear correlation is observed. Although the number

of reported linear relations of the type $^{n}\Delta X = a + b\delta_X$ is small, more examples will come to light as systematic studies are carried out. A less-expected correlation is the linear plot $^{2,3}\Delta C(^{2/1}H) = a + b\delta_{NH_2}(^{1}H)$ in a series of aniline derivatives.[120] Here too the slope b is positive.

A linear correlation has also been observed between isotope shifts and the coupling constant along the same path between the observed nucleus and the point of substitution e.g., $^{1}\Delta^{31}P(^{18/16}O)$ vs $^{1}J(PO)$,[121] $^{1}\Delta^{19}F(^{13/12}C)$ vs $^{1}J(CF)$ in fluoromethanes,[100, 122] $^{2}\Delta^{19}F(^{2/1}H)$ vs $^{2}J(FCH)$ and $^{3}\Delta^{19}F(^{2/1}H)$ vs $^{3}J(FCCH)$ (trans) in fluoroethenes[98] show linear plots. The magnitudes of the isotope shifts increase with increasing mangitude of the coupling constant. There is a recent report which shows just the opposite trend, i.e., the magnitudes of $^{1}\Delta^{13}C(^{2/1}H)$ *decrease* linearly with increasing $^{1}J(CD)$ in methylbenzenes.[123]

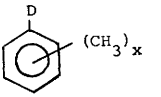

This is somewhat surprising, but small differences in electronic effects may be involved here; the coupling constants only vary by 5% for the entire set of 20 compounds , and the isotope shift varies from – 0.274 to – 0.340 ppm, whereas the other correlations involved wider ranges of values of shifts and couplings. The methylbenzenes are such a closely related set of compounds that methyl group increments on the isotope effects can be discerned. A linear equation for $^{n}\Delta^{13}C(^{2/1}H)$ for various *n* (1 up to 4) in terms of empirical parameters for methyl substituents at *ortho*, *meta*, and *para* positions relative to the observed ^{13}C fit the data if additional parameters representing steric corrections are included.[123]

The ^{13}C-isotope shifts via intramolecular hydrogen bonding paths have been studied in aromatic carbonyl compounds with an *o*-hydroxy group, and in β-keto esters,[124] and in aniline derivatives.[120]

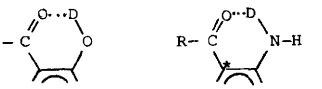

In both structural types the isotope shift is induced via a CO•••D path, effectively a 2-bond isotope effect in which one of the bonds is a hydrogen bond. These shifts are the usual sign and are – 0.18 to – 0.72 ppm. In the anilines, 3-bond isotope shifts are also observed for ^{13}C at R or at the starred position. It is not surprising that these $^{3}\Delta^{13}C(^{2/1}H)$ values are stereospecific: the magnitudes for ^{13}C anti to the hydrogen bond (up to – 75 ppb) being much larger than syn (up to – 25 ppb).[120]

Stereospecificity is also evident in proton isotope shifts observed in propylene and ethylene ozonides,[125, 126] in which $^{4}\Delta^{1}H(^{2/1}H)$ is

$$trans = |-0.0035 \text{ ppm}| > cis = |-0.0015 \text{ ppm}|.^{125}$$

This ordering is consistent with $^{3}\Delta$ in deuterated styrenes in which larger shifts occur,

$$trans = |-0.012\ \text{ppm}| > cis = |-0.005\ \text{ppm}|.$$

$^3\Delta^{19}F(^{2/1}H)$ in fluoroethenes also showed the same trend, *trans* > *cis*, and correlate with the *trans* and the *cis* substituent effects.[98] These observations further support the idea that these 2, 3, 4-bond isotope shifts depend on the secondary derivatives multiplied by a primary dynamic factor, i.e.,

$$(\partial\sigma^F/\partial\Delta r_{CH})_e \bullet (\langle\Delta r\rangle_{CH} - \langle\Delta r\rangle_{CD})$$

or in terms of derivatives of σ^H for proton isotope shifts. Exo-endo stereospecificity is also noted, although the differences are much smaller (– 0.019 ppm vs. – 0.021 ppm) in deuterated bicycloheptanones.[126]

^{13}C isotope shifts in various norbornenyl systems

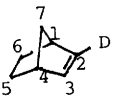

are of the usual sign for the nominally 1-, 2-, and 3-bond isotope shifts at carbons number 1, 2, 3, and 4, but unusual signs for the isotope shifts at carbons 5, 6, and 7. Although it makes little sense to talk of number of bonds between ^{13}C and D in these multipath systems, the isotope shifts observed at carbons 5, 6, or 7 are effectively ($^4\Delta + {}^4\Delta$) or ($^3\Delta + {}^5\Delta$) or ($^3\Delta + {}^4\Delta$). A correlation of the magnitude of the isotope shift against the ^{13}C chemical shift is found for C_7 but not for others.[127] The one-bond ^{15}N- and ^{13}C-induced ^{13}C isotope shifts in pyridine have the usual sign and are about – 17 to – 24 ppb. Much smaller isotope shifts of both signs are also observed over several bonds.[128]

Shifts that are measured between a solute in H_2O and the same solute in D_2O are not strictly intrinsic isotope shifts. The shifts obtained in this way contain not only the intrinsic isotope shift but also shifts due to differences in solvent structure between pure H_2O solvent and pure D_2O solvent. Unlike the intrinsic isotope shift, the solvent effects are highly temperature- and counter-ion-dependent. Unfortunately, these results are hardly ever extrapolated to zero ionic streength or to infinite dilution. Nevertheless, it is worth noting how large are the shifts due to differences in solvent structure, etc. (one might call these isotopic solvent shifts). For example, $^1\Delta^{19}F(^{2/1}H)$ measured in HF and DF gas is – 2.5 ppm, according to Hindermann and Cornwell.[129] In the HF/H_2O solution the shifts are – 5.8 ppm and – 6.2 ppm in 1 *M* and 4 *M* solution,[130] indicating that a large part of what is observed is due to the isotopic solvent shifts. In these HF solutions most of the ^{19}F nuclei observed are in HF environments, and the shifts measure differences between $(HF)(H_2O)_x$ and $(DF)(D_2O)_x$. In the KF solutions, however, the ^{19}F nuclei are primarily in $[F(H_2O)_x]^-$ or $[F(D_2O)_x]^-$ environments. In KF solution in H_2O/D_2O apparent isotope shifts of – 2.86 ppm and – 3.0 ppm are observed in 1 *M* and 0.5 *M* solutions. Solvated Cl^- ion shows apparent ^{37}Cl isotope shifts which are – 4.6 to – 4.7 ppm and ^{35}Cl shifts are – 5.5 ppm. Unfortunately, the reported shifts in this paper were not determined in the limit of infinite dilution or zero ionic strength. The

most puzzling results, if real, are for ^{31}P in $OP(OH)_3$, $O_2P(OH)_2^-$, and $O_3P(OH)^{2-}$ in H_2O relative to $OP(OD)_3$, $O_2P(OD)_2^-$, and $O_3P(OD)^{2-}$ in D_2O, respectively. These shifts are reported to be – 0.15 ppm, – 0.04 ppm, and – 0.16 ppm.[130] There is no obvious explanation for these relative magnitudes which correspond to – 0.05, – 0.02, – 0.16 ppm per deuterium, respectively.

D. Intramolecular and Intermolecular Effects on Nuclear Shielding. — The observed ^{13}C chemical shift differences between the equatorial and the axial conformational isomers of methylcyclohexane (and other molecules) can be considered in terms of additive intramolecular (steric) contributions such as the normal γ-gauche effect and the effect of anti H–H interactions. The presence of anti-related vicinal hydrogens contributes a downfield shift to each of the carbons bearing the hydrogen atoms involved.[131] In epoxides an additional guache γ parameter is deemed necessary.[132] These chemical shift differences between conformers are best observed in the solid state, where ^{13}C signals from individual conformations are observed rather than some average values among several rapidly converting conformers.[133] Calculations of these steric effects on ^{13}C shielding (and also ^{31}P, ^{15}N, ^{17}O, ^{19}F shielding)[134, 135] have been reviewed (this series, Vol. 16, Chapter 1). More recently a different approach using a polarization propagator formalism at the RPA level using GIAO-INDO functions is used to calculate ^1H shifts due to steric effects.[136]

Calculations of shielding in paramagnetic systems have been reported.[137-142] The ^{13}C and ^1H shielding in vanadocene observed as a function of temperature are calculated in terms of the fine structure of the electronic ground state, spin densities at the ligand nuclei, and bond extension with increasing temperature.[137] The effective electron spin density at the ligand nucleus arises from the polarization of the paired ligand electrons by the spin density of the vanadium d^3 electrons. The chemical shifts in a $4d^1$ system,[138, 139] $3d^1$ system,[140-141] and $3d^2$ system[142] in strong crystal fields of various symmetries are calculated as a function of the distance of the observed nucleus from the paramagnetic ion and the temperature using a nonmultipole expansion method.

E. Absolute Shielding Scales. — Refinements to the ^{13}C shielding scale have been reported.[143] ^{13}C chemical shifts in over twenty molecules have been measured relative to ^{13}CO in the zero-pressure limit. Rovibrational averaging effects on the spin rotation constant in $^{13}C^{16}O$ have been used to find

$$\sigma_e(^{13}C \text{ in } ^{13}C^{16}O) = 3.0 \pm 1.2 \text{ ppm}$$
$$\sigma_0\ (^{13}C \text{ in } ^{13}C^{16}O) = 1.0 \pm 1.2 \text{ ppm}.$$

The absolute ^{13}C shieldings so obtained in various molecules are compared with recent very good calculations.

When a nucleus relaxes entirely by the spin-rotation mechanism, then the spin

lattice relaxation rate is directly proportional to C^2_{eff}, which is $C_\perp{}^2$ for linear molecules and $C^2_{iso} + (4/45)\,(\Delta C)^2$ in spherical tops. **C** stands for the spin-rotation tensor. Thus, the simultaneous measurement of T_1 *in the gas phase* for 2 nuclei in the same molecule, both relaxing entirely by the SR mechanism, yields the ratio of C^2_{eff} for the nuclei. In SeF_6 and TeF_6 molecules C is known for the ^{19}F nuclei by independent solid-state NMR measurements.[144] Thus it becomes possible to determine C_{iso} for ^{77}Se and ^{125}Te in these molecules. From the well-known relationship between the SR constant and the paramagnetic shielding:

$$\sigma^{SR} = (m_p / 2mg_k)\ \frac{1}{3} \sum_{\alpha=x,y,z} \frac{C^{(k)}_{\alpha\alpha}}{B_\alpha} \tag{24}$$

$$\sigma^{p} = \sigma^{SR} - \left(\frac{\mu_0}{4\pi}\right) \cdot \frac{e^2}{3m} \sum_{N'} \frac{Z_{N'}}{r_{N'}} \tag{25}$$

$$\sigma^{d} \cong \sigma(\text{free atom}) + \left(\frac{\mu_0}{4\pi}\right) \cdot \frac{e^2}{3m} \sum_{N'} \frac{Z_{N'}}{r_{N'}} \tag{26}$$

so that

$$\sigma \cong \sigma(\text{free atom}) + \sigma^{SR}. \tag{27}$$

For ^{77}Se and ^{125}Te in SeF_6 and TeF_6, **C** is isotropic, and one then only needs the nuclear g value and the rotational constant of the molecule. Thus the ^{77}Se and the ^{125}Te absolute shielding scales were determined.[143]

$$\sigma(^{77}SeF_6) - \sigma(\text{free Se atom}) = -1860 \pm 64 \text{ ppm}$$
$$\sigma(^{125}TeF_6) - \sigma(\text{free Te atom}) = -2790 \pm 130 \text{ ppm}.$$

If we use the free-atom values 3298 ppm (Se) and 6580 ppm (Te), respectively, corrected for relativistic effects, then the rovibrationally averaged absolute shielding in the isolated molecules is

$$\sigma(^{77}SeF_6) = 1438 \text{ ppm}$$
$$\sigma(^{125}TeF_6) = 3790 \text{ ppm}.$$

For the standard liquid reference,

$$\sigma(^{77}SeMe_2, \text{liq}) = 2069 \text{ ppm}$$

was also obtained by measuring the chemical shifts relative to SeF_6 gas. From chemical shift tables, ^{77}Se and ^{125}Te absolute shielding in various molecules can be obtained. For example,

$$\sigma(^{125}TeMe_2 \text{ liq}) \cong 4333 \text{ ppm}.$$

An estimate of the spin rotation constant can also be deduced from liquid state T_1 measurements, but this is much less accurate since other mechanisms generally contribute and the reorientational correlation times in liquids have to be estimated by resorting to models.

The ^{205}Tl absolute shielding scale reported recently[145] is based on the anisotropy of the shielding tensor. If the shielding anisotropy of a linear molecule is known

(from solid state NMR measurements, for example), the absolute isotropic shielding is given by

$$\sigma_{iso} = -\frac{2}{3}\Delta\sigma + \sigma^{d}_{//} \quad \text{(linear)} \tag{28}$$

In Flygare's model,[18]

$$\sigma^{d}_{//} = \sigma(\text{free atom}) + \left(\frac{\mu_0}{4\pi}\right)\cdot\frac{e^2}{2m}\sum_{N'} Z_{N'}\left(\frac{x^2+y^2}{R^3}\right)_{N'} + \text{atom-dipole corrections} \tag{29}$$

Thus,

$$\sigma_{iso} - \sigma(\text{free atom}) \cong -\frac{2}{3}\Delta\sigma + \left(\frac{\mu_0}{4\pi}\right)\cdot\frac{e^2}{2m}\sum_{N'} Z_{N'}\left(\frac{x^2+y^2}{R^3}\right)_{N'} \tag{30}$$

This expression holds only for linear molecules where $\sigma^{p}_{//} = 0$. For a quasi-linear system,

$$\sigma_{iso} = -\frac{2}{3}\Delta\sigma + \sigma^{p}_{//} + \sigma^{d}_{//} \quad .$$

In $[TlMe_2]^+$ ion there are off-axis hydrogens which should give rise to $\sigma^{p}_{//} \neq 0$. For example, off-axis hydrogens in $CH_2{=}^{13}C{=}CH_2$ give rise to a very sizeable $\sigma^{p}_{//}$ ($\cong$ –250 ppm) for the central ^{13}C![146] Forster et al. neglected this and took $\sigma^{p} \cong -(2/3)\Delta\sigma$ for this quasi-linear molecule. The shielding anisotropy in this case was obtained from the CSA contribution to the relaxation rate (assumed to be CSA + SR mechanisms). They further neglected a portion of the diamagnetic part to get

$$\sigma_{iso}(^{205}Tl \text{ in } [TlMe_2]^+_{aq}) - \sigma(\text{free atom}) \cong -(2/3)\Delta\sigma = -3700 \text{ ppm}.$$

We estimate the neglected diamagnetic term is 37.6 ppm in this case, indeed small compared to –3700 ppm. There is a more serious problem. The value of $\Delta\sigma$ deduced from T_1 in this work (5550 ppm) is substantially different from the values measured directly from the powder spectrum of Me_2TlBr ($\Delta\sigma$ = 485 ppm) and Me_2TlNO_3 ($\Delta\sigma$ = 1975 ppm).[147] Thus, the ^{205}Tl absolute shielding scale is still not established.

References

1 P. Lazzeretti and R. Zanasi, *Phys. Rev.* A, 1986, **33**, 3727
2 N.F. Ramsey, *Phys. Rev. A*, 1970, **1**, 1320
3 A. L. Barra, J. B. Robert, and L. Wiesenfeld, *Phys. Lett. A*, 1986, **115**, 443.
4 C. J. Jameson, in *Nuclear Magnetic Resonance* (Specialist Periodical Reports), The Royal Society of Chemistry, London, 1981, Vol. **10**, Chapter 1.
5 D. K. Dalling, R. J. Pugmire, D. M. Grant, and W. E. Hull, *Magn. Reson. Chem.*, 1986, **24**, 191.
6 H. Fukui, *Magn. Reson. Rev.*, 1987, **11**, 205.
7 G. A. Webb, *NATO ASI Ser., Ser. C*, (*NMR of Living Systems*) 1986, **164**, 19
8 N. C. Pyper and P. P. Edwards, *J. Am. Chem. Soc.*, 1986, **108**, 78.
9 R. Tabeta, M. Aida, and H. Saito, *Bull. Chem. Soc. Jpn.*, 1986, **59**, 1957.
10 P. Lazzeretti and J. A. Tossell, *J. Phys. Chem.*, 1987, **91**, 800.
11 J. A. Tossell and P. Lazzeretti, *J. Chem. Phys.*, 1987, **86**, 4066
12 D. B. Chesnut and C. K. Foley, *J. Chem. Phys.*, 1986, **85**, 2814
13 R. Höller and H. Lischka, *Mol. Phys.*, 1980. **41**, 1041.

14 P. Lazzeretti and R. Zanasi, *J. Chem. Phys.*, 1980, **72**, 6768
15 F. Keil and R. Ahlrichs, *J. Chem. Phys.*, 1979, **71**, 2671.
16 F. H. deLeeuw and A. Dymanus, *J. Mol. Spectrosc.*, 1973, **48**, 427.
17 E. W. Kaiser, *J. Chem. Phys.*, 1970, **53**, 1686.
18 T. D. Gierke and W. H. Flygare, *J. Am. Chem. Soc.*, 1972, **94**, 7277.
19 R. E. Wasylishen, C. Connor, and J. O. Friedrich, *Can. J. Chem.*, 1984, **62**, 981.
20 P. B. Davies, R. M. Neumann, S. C. Wofsy, and W. Klemperer, *J. Chem. Phys.*, 1971, **55**, 3564.
21 N. Zumbulyadis and B. P. Dailey, *Mol. Phys.*, 1974, **27**, 633.
22 G. Malli and C. Froese, *Int. J. Quantum Chem.*, 1967, **1S**, 95.
23 J. Raymonda and W. Klemperer, *J. Chem. Phys.*, 1971, **55**, 232.
24 A. J. Montana, N. Zumbulyadis, and B. P. Dailey, *J. Chem. Phys.*, 1976, **65**, 4756.
25 L. Maier, *J. Chem. Soc., Chem. Commun.*, **1969**, 961.
26 B. R. Appleman and B. P. Dailey, *Adv. Magn. Reson.*, 1974, **7**, 231.
27 H. Siebert, J. Eints, and E. Fluck, *Z. Naturforsch. B*, 1968, **23**, 1006.
28 G. Heckmann and E. Fluck, *Z. Naturforsch. B*, 1969, **24**, 1092.
29. H. W. Spiess, R. Grosescu, and U. Haeberlen, *Chem. Phys.*, 1974, **6**, 226.
30. G. S. Reddy and R. Schmutzler, *Z. Naturforsch. B*, 1970, **25**, 1199.
31. A. R. Grimmer and U. Haubenreisser, *Chem. Phys. Lett.*, 1983, **99**, 487.
32 J. A. Tossell and P. Lazzeretti, *Chem. Phys. Lett.*, 1986, **128**, 420.
33. R. Höller and H. Lischka, *Mol. Phys.*, 1980, **41**, 1017.
34 M. Schindler and W. Kutzelnigg, *J. Chem. Phys.*, 1982, **76**, 1919.
35 U. Niemann and H. C. Marsmann, *Z. Naturforsch. B*, 1975, **30**, 202.
36 H. Marsmann, in *NMR Basic Principles and Progress*, Vol. **17**, eds. P. Diehl, E. Fluck, and R. Kosfeld (Springer, Berlin, 1981) p. 65.
37 K. W. Zilm, D. M. Grant, J. Michl, M. J. Fink, and R. West, *Organometallics*, 1983, **2**, 193.
38 J. A. Tossell and P. Lazzeretti, *Chem. Phys. Lett.*, 1986, **132**, 464.
39 J. A. Tossell and P. Lazzeretti, *J. Chem. Phys.*, 1986, **84**, 369.
40. R. Radeglia, *Z. Naturforsch. B*, 1977, **32**, 1091; *Z. phys. Chem. (Leipzig)*, 1975, **256**;, 453; G. Engelhardt, R. Radeglia, H. Jancke, E. Lippmaa, and M. Mägi, *Org. Magn. Reson.*, 1973, **5**, 561.
41 J. A. Tossell and P. Lazzeretti , *J. Phys. B*, 1986, **19**, 3217.
42 P. Lazzeretti and J. A. Tossell, *J. Magn. Reson.*, 1986, **70**, 461.
43 C. J. Jameson, A. K. Jameson, and P. M. Burrell, *J. Chem. Phys.*, 1980, **73**, 6013.
44 S. C. Wofsy, J. S. Muenter, and W. Klemperer, *J. Chem. Phys.*, 1971, **55**, 2014.
45 J. A. Courtney and R. L. Armstrong, *Can. J. Phys.*, 1971, **50**, 1252.
46 I. Ozier, L. M. Crapo, and S. S. Lee, *Phys. Rev.*, 1968, **172**, 63.
47 J. Mason, *J. Chem. Soc., Dalton Trans.*, **1975**, 1426.
48 J. C. Facelli, D. M. Grant, and J. Michl, *Acc. Chem. Res.*, 1987, **20**, 152.
49 J. C. Facelli, D. M. Grant, and J. Michl, *Int. J. Quantum Chem.*, 1987, **31**, 45.
50 J. C. Facelli, A. M. Orendt, M. S. Solum, G. Depke, D. M. Grant, and J. Michl, *J. Am. Chem. Soc.*, 1986, **108**, 4268.
51 M. S. Solum, J. C. Facelli, J. Michl, and D. M. Grant, *J. Am. Chem. Soc.*, 1986, **108**, 6464.
52 C. J. Jameson and H. J. Osten, *Mol. Phys.*, 1985, **56**, 1083.
53 C. J. Jameson and H. J. Osten, *J. Chem. Phys.*, 1985, **83**, 5425.
54 J. C. Facelli, A. M. Orendt, A. J. Beeler, M. S. Solum, D. Depke, K. D. Malsch, J. W. Downing, P. S. Murthy, D. M. Grant, and J. Michl, *J. Am. Chem. Soc.*, 1985, **107**, 6749.
55 B. L. Poh, *Magn. Reson. Chem.*, 1986, **24**, 816.
56 R. Pachter and P. L. Wessels, *J. Mol. Struct.*, THEOCHEM, 1986, **30**, 143.
57 B. Eliasson, U. Edlund, and K. Muellen, *J. Chem. Soc., Perkin Trans. 2*, **1986**, 937.
58 W. P. Dailey, *Tetrahedron Lett.*, 1986, **27**, 2825.
59 A. Battais, G. Bauduin, B. Boutevin, and Y. Pietrasanta, *J. Fluorine Chem.*, 1986, **31**, 197.
60 R. Bramley, M. Brorson, A. M. Sargeson, and C. E. Schäffer, *J. Am. Chem. Soc.*, 1985, **107**, 2780.

61 N. Juranic, *J. Magn. Reson.*, 1987, **71**, 144.
62 R. Bramley, M. Brorson, A. M. Sargeson, and C. E. Schäffer, *Inorg. Chem.*, 1987, **26**, 314.
63 A. D. Buckingham and P. J. Stephens, *J. Chem. Soc.*, **1964**, 2747, 4583.
64 H. Nakatsuji, K. Kanda, K. Endo, and T. Yonezawa, *J. Am. Chem. Soc.*, 1984, **106**, 453.
65 K. Kanda, H. Nakatsuji, and T. Yonezawa, *J. Am. Chem. Soc.*, 1984, **106**, 5888.
66 H. McConnell, *J. Chem. Phys.*, 1957, **27**, 226.
67 J. A. Pople, *J. Chem. Phys.*, 1962, **37**, 53.
68 N. Jouini, *J. Solid State Chem.*, 1986, **63**, 439.
69 J. R. Ascenso, R. K. Harris, and P. Granger, *Organomet. Chem.*, 1986, **301**, C23.
70 R. K. Harris and K. J. Packer, *J. Chem. Soc., Dalton Trans.*, **1986**, 1015.
71 C.T.G. Knight, G. L. Turner, R. J. Kirkpatrick, and E. Oldfield, *J. Am. Chem. Soc.*, 1986, **108**, 7426.
72 J. Jokisaari and T. Vaananen, *Mol. Phys.*, 1986, **58**, 959.
73 P. S. Marchetti, R. S. Honkonen, and P. D. Ellis, *J. Magn. Reson.*, 1987, **71**, 294.
74 R. S. Honkonen and P. D. Ellis, *J. Am. Chem. Soc.*, 1984, **106**, 5488.
75 L. Baltzer, *J. Am. Chem. Soc.*, 1987, **109**, 3479.
76 U. Haubenreisser, U. Sternberg, and A. R. Grimmer, *Mol. Phys.*, 1987, **60**, 151.
77 L. Griffiths, A. Root, R. K. Harris, K. J. Packer, A. M. Chippendale, and F. R. Tromans, *J. Chem. Soc., Dalton Trans.*, **1986**, 2247.
78 G. L. Turner, K. A. Smith, J. R. Kirkpatrick, and E. Oldfield, *J. Magn. Reson.*, 1986, **70**, 408.
79 N. J. Clayden, C. M. Dobson, L. Y. Lian, and D. J. Smith, *J. Magn. Reson.*, 1986, **69**, 476.
80 A. K. Cheetham, N. J. Clayden, C. M. Dobson, and R.J.B. Jakeman, *J. Chem. Soc., Chem. Commun.*, **1986**, 195.
81 J. Jokisaari, Y. Hiltunen, and J. Lounila, *J. Chem. Phys.*, 1986, **85**, 3198.
82 D. B. Chesnut and C. K. Foley, *J. Chem. Phys.*, 1986, **84**, 852.
83 R. Ditchfield, *Chem. Phys.*, 1973, **2**, 400.
84 K. W. Zilm and D. M. Grant, *J. Am. Chem. Soc.*, 1981, **103**, 2913.
85. M. Schindler and W. Kutzelnigg, *J. Am. Chem. Soc.*, 1983, **105**, 1360.
86 C. L. Khetrapal, S. Raghothama, and N. Suryaprakash, *J. Magn. Reson.*, 1987, **71**, 140.
87 C. M. Carter, D. W. Alderman, J. C. Facelli, and D. M. Grant, *J. Am. Chem. Soc.*, 1987, **109**, 2639.
88 J. A. Pople, *J. Chem. Phys.*, 1962, **37**, 60.
89 P. Lazzeretti, E. Rossi, and R. Zanasi, *J. Chem. Phys.*, 1982, **77**, 3129; 1981, **75**, 5019.
90 B. A. Cornell, *J. Chem. Phys.*,1986, **85**, 4199.
91 L. A. Nafie and T. B. Freedman, *Chem. Phys. Lett.*, 1987, **134**, 225.
92 C. J. Jameson and H. J. Osten, *Ann. Rep. NMR Spectrosc.*, 1986, **17**, 1.
93 D. B. Chesnut, *Chem. Phys.*, 1986, **110**, 415.
94 R. Ditchfield, *Chem. Phys.*, 1981, **63**, 185.
95 R. M. Stevens, R. M. Pitzer, and W. N. Lipscomb, *J. Chem. Phys.*, 1963, **38**, 550.
96 R. M. Stevens and W. N. Lipscomb, *J. Chem. Phys.*, 1964, **40**, 2238.
97 H. J. Osten and C. J. Jameson, *J. Chem. Phys.*, 1984, **81**, 4288.
98 H. J. Osten, C. J. Jameson, and N.C. Craig, *J. Chem. Phys.*, 1985, **83**, 5434.
99 C. J. Jameson, D. Rehder, and M. Hoch, *J. Am. Chem. Soc.*, 1987, **109**, 2589.
100 C. J. Jameson and H. J. Osten, *Mol. Phys.*, 1985, **55**, 383.
101 C. J. Jameson, A. K. Jameson, and D. Oppusunggu, *J. Chem. Phys.*, 1986, **85**, 5480.
102 C. J. Jameson and A. K.Jameson, *J. Chem. Phys.*, 1986, **85**, 5484.
103 C. J. Jameson, *J. Am. Chem. Soc.*, 1987, **109**, 2586.
104 C. J. Jameson, A. K. Jameson, and H. Parker, *J. Chem. Phys.*, 1979, **70**, 5916.
105 C. J. Jameson, A. K. Jameson, and D. Oppusunggu, *J. Chem. Phys.*, 1984, **81**, 85.
106 G. B. Benedek, R. Englman, and J. A. Armstrong, *J. Chem. Phys.*, 1963, **39**, 3349.
107 W. S. Jung, H. Tomiyasu, and H. Fukutomi, *Bull. Chem. Soc. Jpn.*, 1986, **59**, 3761.

108 M. Hoch and D. Rehder, *Inorg. Chim. Acta*, 1986, **111**, L13.
109 T. Schaefer, J. Peeling, and G. H. Penner, *Can. J. Chem.*, 1986, **64**, 2162.
110 A. Pulkkinen, J. Jokisaari, and T. Vaananen, *J. Mol. Struct.*, 1986, **144**, 359.
111 D. A. Forsyth, J. S. Puckace, and F. E. Shawcross, *Tetrahedron Lett.*, 1986, **27**, 3569.
112 J. W. Timberlake, J. A. Thomson, and R. W. Taft, *J. Am. Chem. Soc.*, 1971, **93**, 274.
113 C. J. Jameson and H. J. Osten, *J. Chem. Phys.*, 1984, **81**, 4293.
114 S. Aime, E. Santucci, and R. Fruttero, *Magn. Reson. Chem.*, 1986, **24**, 919.
115 O. Lutz and H. Oehler, *Z. Naturforsch. A*, 1977, **32**, 131.
116 W. T. Raynes, *Mol. Phys.*, 1983, **49**, 443.
117 C. J. Jameson, *Mol. Phys.*, 1985, **54**, 73.
118 J. R. Everett, *Org. Magn. Reson.*, 1982, **19**, 86.
119 C. H. Arrowsmith and J. A. Kresge, *J. Am. Chem. Soc.*, 1986, **108**, 7918.
120 J. Reuben, *J. Am. Chem. Soc.*, 1987, **109**, 316.
121 R. D. Sammons, P. A. Frey, K. Bruzik, and M. D. Tsai, *J. Am. Chem. Soc.*, 1983, **105**, 5455.
122 S. G. Frankiss, *J. Phys. Chem.*, 1963, **67**, 752.
123 S. Berger and B.W.K. Diehl, *Magn. Reson. Chem.*, 1986, **24**, 1073.
124 P. E. Hansen, *Magn. Reson. Chem.*, 1986, **24**, 903.
125 J. I. Choe, H. S. Choi, and R. L. Kuczkowski, *Magn. Reson. Chem.*, 1986, **24**, 1044.
126 N. H. Werstiuk, G. Timmins, and B. Sayer, *Can. J. Chem.*, 1986, **64**, 1465.
127 H. Künzer, C. E. Cottrell, and L. A. Paquette, *J. Am. Chem. Soc.*, 1986, **108**, 8089.
128 S. R. Maple and A. Allerhand, *J. Am. Chem. Soc.*, 1987, **109**, 56.
129 D. K. Hindermann and C. D. Cornwell, *J. Chem. Phys.*, 1968, **48**, 2017.
130 R. M. Jarret and M. Saunders, *J. Am. Chem. Soc.*, 1986, **108**, 7549.
131 J. K. Whitesell and M. A. Minton, *J. Am. Chem. Soc.*, 1987, **109**, 225.
132 M. I. Colombo, D. A. Bustos, M. Gonzalez-Sierra, A. C. Olivieri, E. A. Ruveda, *Can. J. Chem.*, 1986, **64**, 552.
133 H. Saito, *Magn. Reson. Chem.*, 1986, **24**, 835.
134 S. Li and D. B. Chesnut, *Magn. Reson. Chem.*, 1986, **23**, 625; **24**, 93.
135 D. B. Chesnut and W. P. Johnson, *J. Magn. Reson.*, 1985, **65**, 110.
136 M. B. Ferraro, M. A. Natiello, and R. H. Contreras, *Int. J. Quantum Chem.*, 1986, **30**, 77.
137 H. Eicher, F. H. Koehler, and R. Cao, *J. Chem. Phys.*, 1987, **86**, 1829.
138 S. Ahn, S. W. Oh, and S. W. Ro, *Bull. Korean Chem. Soc.*, 1986, **7**, 170.
139 S. Ahn, S. W. Oh, and J. S. Ko, *Bull. Korean Chem. Soc.*, 1986, **7**, 249.
140 S. Ahn, D. H. Kim, and C. J. Choi, *Bull. Korean Chem. Soc.*, 1986, **7**, 299.
141 S. Ahn and K. H. Lee, *Bull. Korean Chem. Soc.*, 1986, **7**, 246.
142 S. Ahn and K. H. Lee, *J. Magn. Reson.*, 1986, **68**, 499.
143 A. K. Jameson and C. J. Jameson, *Chem. Phys. Lett.*, 1987, **134**, 461.
C. J. Jameson and A. K. Jameson, *Chem. Phys. Lett.*, 1987, **135**, 254.
144 S. K. Garg, J. A. Ripmeester, and D. W. Davidson, *J. Magn. Reson.*, 1980, **39**, 317.
145 M. J. Forster, D. G. Gillies, and R. W. Matthews, *Mol. Phys.*, 1987, **160**, 129.
146 A. J. Beeler, A. M. Orendt, D. M. Grant, P. W. Cutts, J. Michl, K. W. Zilm, J. W. Downing, J. C. Facelli, M. S. Schindler, and W. Kutzelnigg, *J. Am. Chem. Soc.*, 1984, **106**, 7672.
147. J. F. Hinton and K. R. Metz, *J. Magn. Reson.*, 1983, **53**, 131.